Inorg. Chem. **2008**, *47*, 11129−11142

Cyclometalated Platinum(II) Complexes of Pyrazole-Based, N^C^N-Coordinating, Terdentate Ligands: the Contrasting Influence of Pyrazolyl and Pyridyl Rings on Luminescence

Stéphanie Develay, Octavia Blackburn, Amber L. Thompson, and J. A. Gareth Williams*

Department of Chemistry, University of Durham, Durham, DH1 3LE, U.K.

Received July 29, 2008

1,3-Bis(1-pyrazolyl)-5-methyl-benzene, HL^2, undergoes cyclometalation at the C^2 position upon reaction with K_2PtCl_4, to generate an N^C^N-coordinated complex, PtL^2Cl. This compound is luminescent in degassed solution at 298 K, emitting in the blue region of the spectrum on the microsecond time scale ($\lambda_{max} = 453$ nm, $\tau = 4.0$ μs, $\Phi_{lum} = 0.02$, in CH_2Cl_2). Compared to the analogous complex Pt(dpyb)Cl that incorporates pyridyl rather than pyrazole rings {dpybH = 1,3-di(2-pyridyl)-benzene}, the excited state is displaced to higher energy by 1700 cm^{-1}. This effect is rationalized in terms of the poorer π-acceptor nature of pyrazolyl compared to pyridyl rings, leading to destabilization of the lowest unoccupied molecular orbital, which is largely localized on the heteroaromatic rings in both cases. Cyclic voltammetry and density functional theory calculations reinforce this interpretation, and suggest that the lowest-energy excited state is probably best described as heavily mixed $\pi_L/d_{Pt}/p_{Cl} \rightarrow \pi^*_L$ (IL/MLCT/LLCT) in character. 5-Aryl-substituted analogues of HL^2 are accessible in three steps from 1,3,5-tribromobenzene by Pd-catalyzed cross-coupling with aryl boronic acids, followed by copper-catalyzed bromo-iodo exchange, and subsequent amination with pyrazole under relatively mild conditions also catalyzed by copper. The corresponding Pt(II) complexes display red-shifted and more intense luminescence compared to PtL^2Cl. Ligands incorporating one pyrazole and one pyridyl ring are also accessible; for example, 1-(1-pyrazolyl)-3-(2-pyridyl)benzene, HL^6. Their complexes are highly luminescent in solution; for example, for PtL^6Cl, $\lambda_{max} = 487$ nm, $\tau = 6.9$ μs, $\Phi_{lum} = 0.55$, in dilute solution in CH_2Cl_2. At elevated concentrations, PtL^6Cl displays an additional excimeric emission band that is substantially blue-shifted compared to that displayed by Pt(dpyb)Cl (bands centered at 645 and 695 nm, respectively), indicating that the presence of the pyrazole ring destabilizes the excimer. The introduction of a methyl substituent into the central aryl ring of such complexes is sufficient to eliminate the excimer emission.

Introduction

Over the past 15 years, several families of platinum(II) complexes have been developed that display photoluminescence in solution at room temperature.[1] A strategy for promoting emission over non-radiative decay has emerged, namely to ensure that d-d excited states involving the population of the strongly antibonding $d_{x^2-y^2}$ orbital are not thermally accessible to the emissive state. It is the thermally activated population of such distorted states that accounts for the lack of room temperature emission in simple complexes like $Pt(bpy)Cl_2$ and $[Pt(tpy)Cl]^+$.[1,2] The key to raising the energy of the d-d states is to introduce strong-field ligands or co-ligands. For example, a wide range of luminescent complexes have been obtained by using acetylide co-ligands in complexes of the general type $Pt(N^N)(-C\equiv CR)_2$ and $[Pt(N^N^N)(-C\equiv CR)]^+$ (where N^N and N^N^N represent di- and tri-imine ligands such as bipyridine and terpyridine),[1d,e,3] while cyclometalating ligands such as 2-phenylpyridine and 6-phenyl-2,2′-bipyridine have a beneficial effect on luminescence quantum yields compared to

* To whom correspondence should be addressed. E-mail: j.a.g.williams@durham.ac.uk.

(1) For recent reviews, see for example: (a) McMillin, D. R.; Moore, J. J. *Coord. Chem. Rev.* **2002**, *229*, 113. (b) Lai, S. W.; Che, C. M. *Top. Curr. Chem.* **2004**, *241*, 27. (c) Ma, B.; Djurovich, P.; Thompson, M. E. *Coord. Chem. Rev.* **2005**, *249*, 1501. (d) Castellano, F. N.; Pomestchenko, I. E.; Shikhova, E.; Hua, F.; Muro, M. L.; Rajapakse, N. *Coord. Chem. Rev.*, **2006**, *250*, 1819. (e) Wong, K. M. C.; Yam, V. W. W. *Coord. Chem. Rev.* **2007**, *251*, 2477. (f) Williams, J. A. G. *Top. Curr. Chem.* **2007**, *281*, 205.

(2) Barigelletti, F.; Sandrini, D.; Maestri, M.; Balzani, V.; von Zelewsky, A.; Chasot, L.; Jolliet, P.; Maeder, U. *Inorg. Chem.* **1988**, *27*, 3644.

10.1021/ic8014157 CCC: $40.75
Published on Web 11/01/2008

complexes with their non-cyclometalated cousins bpy and tpy.[4,5] Potential applications range from chromophores for promoting photoinduced charge separation for artifical photosynthesis,[6] to triplet emitters in organic light-emitting devices (OLEDs).[7,8]

Among metal complexes, a feature essentially unique to square planar d^8 systems is their coordinative unsaturation, which allows them to engage in intermolecular interactions that involve either metal orbitals orthogonal to the plane of the molecule or overlap of cofacial ligand orbitals. Such interactions include the formation of excimers, which may themselves be emissive. If the excimer and monomer emissions between them span the bulk of the visible spectrum, this effect can provide a means of obtaining single-dopant white-light OLEDs.[7a,d,8]

We have been exploring the chemistry and applications of a family of brightly emissive cyclometalated platinum(II) compounds incorporating N^C^N-coordinating terdentate ligands based on 1,3-di(2-pyridyl)benzene (dpybH) (Scheme 1, generic structure I). As previously reported in this journal, these complexes emit from triplet states with high luminescence quantum yields, {e.g., for R = H, $\Phi_{lum} = 0.6$},[9] and they function efficiently in OLEDs.[10] The emission wavelength is tunable over a wide range by varying the substituent R, without compromising the quantum yield (λ_{max} from 481 nm for R = CO_2Me to 588 nm for $-C_6H_4-NMe_2$ in CH_2Cl_2 solution).[11] At elevated concentrations in solution, the complexes form excimers that emit with unusually high efficiency at around 700 nm ($\Phi_{lum} \sim 0.3$). Neat thin films display emission uniquely in this region, leading to high-performance near-IR OLEDs,[12] while the combination of monomer and excimer emission when doped at appropriate concentrations in polymer matrixes has led to particularly efficient white-light emitting devices.[13] In this contribution, we describe our studies into the synthesis and luminescence properties of a family of compounds, structurally related to Pt(dpyb)Cl, but comprising either one or two pyrazoles (pyz) in place of the pyridine (py) rings (Scheme 1, generic structure II). Given the poorer π-acceptor nature of the pyrazole compared to pyridine ring, we reasoned that the lowest unoccupied molecular orbital (LUMO) energy in such complexes would be raised relative to that in complexes of type-I structure, potentially offering a route to triplet emission in the challenging blue region of the spectrum. We also sought to determine how the switch from py to pyz rings would affect intermolecular interactions, particularly excimer formation. The influence of aryl substituents at position R is considered, and asymmetric systems incorporating one pyz and one py ring (Scheme 1, generic structure III) have been explored.

Scheme 1. Generic Structures of the Pyrazole-Containing Complexes (II and III) and Those Based on 1,3-Dipyridylbenzene (I)

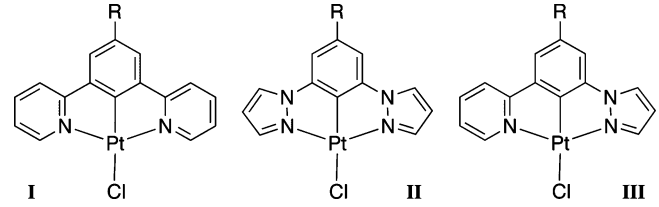

Overview of Binding Modes of Azole-Containing Ligands to Platinum(II). Most of the complexes of pyrazole-containing bidentate ligands reported that are luminescent involve C-linked, 3-substituted pyrazoles: metal complexation is often accompanied by deprotonation at N^2, leading to a strong ligand field.[14,15] For example, 3-(2-pyridyl)-pyrazole can be considered an analogue of the cyclometalating ligand ppyH, if it binds through coordination mode (ii) (Scheme 2,a). Similarly, 1,2,4-triazoles[16] and tetrazoles[17] bind as anionic ligands through N-deprotonation. Chi and co-workers have pioneered the use of such ligands

(3) (a) Chan, C.-W.; Cheng, L.-K.; Che, C.-M. *Coord. Chem. Rev.* **1994**, *132*, 87. (b) Hissler, M.; Connick, W. B.; Geiger, D. K.; McGarrah, J. E.; Lipa, D.; Lachicotte, R. J.; Eisenberg, R. *Inorg. Chem.* **2000**, *39*, 447. (c) Whittle, C. E.; Weinstein, J. A.; George, M. W.; Schanze, K. S. *Inorg. Chem.* **2001**, *40*, 4053. (d) Yam, V. W. W.; Wong, K. M. C. *Top. Curr. Chem.* **2005**, *257*, 1. (e) Rachford, A. A.; Goeb, S.; Ziessel, R.; Castellano, F. N. *Inorg. Chem.* **2008**, *47*, 4348. (f) Lanoë, P.-H.; Fillaut, J.-L.; Toupet, L.; Williams, J. A. G.; Le Bozec, H.; Guerchais, V., *Chem. Commun.* [Online early access]. DOI: 10.1039/b806935b. Published Online: **2008**; in press.

(4) (a) Kvam, P.-I.; Puzyk, M. V.; Balashev, K. P.; Songstad, J. *Acta Chem. Scand.* **1995**, *49*, 335. (b) Mdleleni, M. M.; Bridgewater, J. S.; Watts, R. J.; Ford, P. C. *Inorg. Chem.* **1995**, *34*, 2334. (c) Brooks, J.; Babayan, Y.; Lamansky, S.; Djurovich, P. I.; Tsyba, I.; Bau, R.; Thompson, M. E. *Inorg. Chem.* **2002**, *41*, 3055. (d) Yin, B.; Niemeyer, F.; Williams, J. A. G.; Jiang, J.; Boucekkine, A.; Toupet, L.; Le Bozec, H.; Guerchais, V. *Inorg. Chem.* **2006**, *45*, 8584.

(5) (a) Cheung, T.-C.; Cheung, K.-K.; Peng, S.-M.; Che, C.-M. *J. Chem. Soc., Dalton Trans.* **1996**, 1645. (b) Neve, F.; Crispini, A.; Campagna, S. *Inorg. Chem.* **1997**, *36*, 6150. (c) Lai, S.-W.; Chan, M.C.-W.; Cheung, T.-C.; Peng, S.-M.; Che, C.-M. *Inorg. Chem.* **1999**, *38*, 4046. (d) Wong, K.-H.; Chan, M.C.-W.; Che, C.-M. *Chem.—Eur. J.* **1999**, *5*, 2845. (e) Ma, D.-L.; Che, C.-M. *Chem.—Eur. J.* **2003**, *9*, 6133.

(6) For a review, see: (a) Chakraborty, S.; Wadas, T. J.; Hester, H.; Schmehl, R.; Eisenberg, R. *Inorg. Chem.* **2005**, *44*, 6865.

(7) For example: (a) Adamovich, V.; Brooks, J.; Tamayo, A.; Alexander, A. M.; Djurovich, P. I.; D'Andrade, B. W.; Adachi, C.; Forrest, S. R.; Thompson, M. E. *New J. Chem.* **2002**, *26*, 1171. (b) Lu, W.; Mi, B.-X.; Chan, M.C.-W.; Hui, Z.; Che, C.-M.; Zhu, N.; Lee, S.-T. *J. Am. Chem. Soc.* **2004**, *126*, 4958. (c) Cocchi, M.; Fattori, V.; Virgili, D.; Sabatini, S.; Di Marco, P.; Maestri, M.; Kalinowski, J. *Appl. Phys. Lett.* **2004**, *84*, 1052. (d) He, Z.; Wong, W.-Y.; Yu, X.; Kwok, H.-S.; Lin, Z. *Inorg. Chem.* **2006**, *45*, 10922.

(8) For recent reviews of Pt complexes applied to OLEDs, see: (a) Xiang, H.-F.; Lai, S.-W.; Lai, P. T.; Che, C.-M. Phosphorescent platinum(II) materials for OLED applications. In *Highly efficient OLEDs with phosphorescent materials*; H., Yersin, Ed.; Wiley-VCH: Weinheim, 2008. (b) Williams, J. A. G.; Develay, S.; Rochester, D. L.; Murphy, L. *Coord. Chem. Rev.* [Online early access]. DOI: 10.1016/j.ccr.2008.03.014. Published Online: **2008**; in press.

(9) Williams, J. A. G.; Beeby, A.; Davies, E. S.; Weinstein, J. A.; Wilson, C. *Inorg. Chem.* **2003**, *42*, 8609.

(10) (a) Sotoyama, W.; Satoh, T.; Sawatari, N.; Inoue, H. *Appl. Phys. Lett.* **2005**, *86*, 153505. (b) Cocchi, M.; Virgili, D.; Fattori, V.; Rochester, D. L.; Williams, J. A. G. *Adv. Funct. Mater.* **2007**, *17*, 285. (c) Kalinowski, J.; Cocchi, M.; Virgili, D.; Fattori, V.; Williams, J. A. G. *Chem. Phys. Lett.* **2006**, *432*, 110. (d) *Chem. Phys. Lett.*, **2007**, *447*, 279.

(11) Farley, S. J.; Rochester, D. L.; Thompson, A. L.; Howard, J. A. K.; Williams, J. A. G. *Inorg. Chem.* **2005**, *44*, 9690.

(12) (a) Cocchi, M.; Virgili, D.; Fattori, V.; Williams, J. A. G.; Kalinowski, J. *Appl. Phys. Lett.* **2007**, *90*, 023506. (b) Cocchi, M.; Kalinowski, J.; Virgili, D.; Williams, J. A. G. *Appl. Phys. Lett.* **2008**, *92*, 113302.

(13) (a) Cocchi, M.; Kalinowski, J.; Virgili, D.; Fattori, V.; Develay, S.; Williams, J. A. G. *Appl. Phys. Lett.* **2007**, *90*, 163508. (b) Virgili, D.; Cocchi, M.; Fattori, V.; Sabatini, S.; Kalinowski, J.; Williams, J. A. G. *Chem. Phys. Lett.* **2006**, *433*, 145. (c) Kalinowski, J.; Cocchi, M.; Virgili, D.; Fattori, V.; Williams, J. A. G. *Adv. Mater.* **2007**, *19*, 4000.

(14) For a recent review of pyridyl azolates in the preparation of luminescent complexes, see: (a) Chi, Y.; Chou, P. T. *Chem. Soc. Rev.* **2007**, *36*, 1421.

Scheme 2. (a) Tautomeric Forms of the C-Linked Compound 3-(2-Pyridyl)-pyrazole, Which Can Coordinate to a Metal M Either As a Neutral Ligand Leaving N^1 Protonated (i), or As an Anionic Ligand through Deprotonation (ii). (b) An example of an N-Linked 1-(Aryl)pyrazole. (c) Pt Complexes of the N-Linked, Terdentate Ligand 1,3-Bis(1-pyrazolyl)pyridine (bpp) Have Been Investigated by Connick et al.

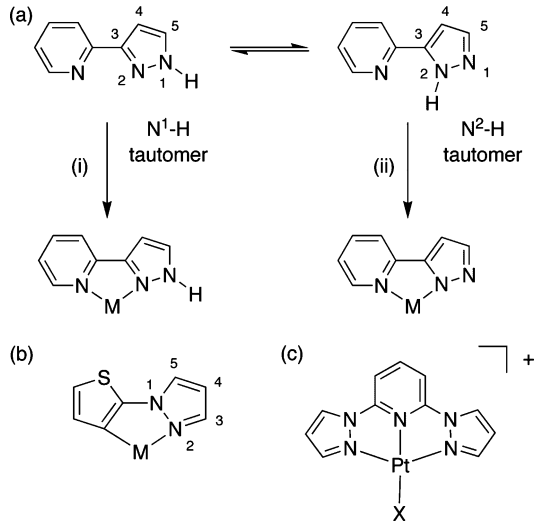

in the design of several luminescent Pt(II) complexes,[15c,18] while a range of Os(II) and Ir(III) complexes have also been reported.[14,15a,b,d,16] N-linked 1-arylpyrazoles that cyclometallate through the aryl ring[19] (Scheme 2,b) featured in some of the earliest examples of room-temperature-emissive Pt(II) complexes; for example, Pt(thpy)(ppz) {thpyH = 2-(2-thienyl)pyridine; ppzH = 1-phenylpyrazole}.[20]

There has been less investigation into the utility of *terdentate* pyrazole-containing ligands. Recently, Lam and co-workers described the intriguing properties of the Pt(II) complex of 6-phenyl-2-(3-pyrazolyl)pyridine (HphppzH).[21] This C-linked pyrazole ligand binds in a cyclometalating, *mono*anionic, C^N^N-coordinating fashion to give Pt(phppzH)Cl, that is, without deprotonation of the pyrazole—the proton remains on the noncoordinated N^1 position, as in binding mode (i), Scheme 2a. However, treatment with base leads to deprotonation and formation of a dimer, $[Pt(\mu\text{-phppz})]_2$, in which N^1 becomes coordinated to a second platinum(II) ion with displacement of the chloride co-ligand. Meanwhile, Connick and co-workers have explored Pt(II) complexes of N-linked, 2,6-bis(1-pyrazolyl)pyridine (bpp, Scheme 2,c),[22] a terpyridine analogue that has been widely explored with other metal ions:[23] emission was only observed at 77 K for the complex $[Pt(bpp)Ph](PF_6)$. Earlier this year, and toward the concluding stages of the work presented herein, Connick also reported on structural aspects of the Pt(II) complex of 1,3-bis(1-pyrazolyl)benzene (Scheme 1: structure II, R = H), the results of which relate directly to our studies, and which are discussed in that context below.[24]

Results and Discussion

Synthesis of Ligands. The complexes studied are shown in Scheme 3, and the strategies employed in the synthesis of the requisite N-linked ligands are summarized in Scheme 4. The formation of aryl-nitrogen bonds is typically catalyzed by copper(I) salts. A wide range of conditions and catalytic species have been explored since the original reports of Ullmann and Goldberg at the beginning of the last century.[25] Our initial preparation of the parent ligand 1,3-bis(1-pyrazolyl)benzene HL^1 was carried out by a modified Ullmann coupling of 1,3-diiodobenzene with an excess of pyrazole, in which the addition of 1,10-phenanthroline as a ligand for Cu(I) facilitates reaction under milder conditions.[26] However, yields were limited to around 20% using this method. Buchwald et al. have recently described how the combination of CuI with chelating aliphatic amines, such as 1,2-diaminocyclohexane, allows N-arylation of a range of N-heterocycles including pyrazoles under mild conditions.[27] This methodology proved superior for the synthesis of HL^1, giving yields of up to 80% (Scheme 4,a). The singly reacted compound 1-iodo-3-(1-pyrazolyl)benzene, *pre-6*, was isolated as a side product.

When applied to the synthesis of HL^2 from 1,3-dibromo-5-methyl-benzene, on the other hand, these conditions led to poor conversion, probably because of the deactivating influence of the methyl group and the lower reactivity of bromo compared to iodo substrates. The latter problem could be overcome by first carrying out a bromo—iodo exchange reaction using NaI as the source of iodide, catalyzed by CuI in the presence of *N*,*N*-dimethyl-1,2-ethylenediamine. Buchwald et al. reported that this catalyst system can offer near-quantitative conversion of monobrominated aromatics to their iodo analogues.[28] In the present instance of a dibrominated

(15) (a) Wu, P.-C.; Yu, J.-K.; Song, Y.-H.; Chi, Y.; Chou, P.-T.; Peng, S.-M.; Lee, G.-H. *Organometallics* **2003**, *22*, 4938. (b) Yang, C.-H.; Li, S.-W.; Chi, Y.; Cheng, Y.-M.; Yeh, Y.-S.; Chou, P.-T.; Lee, G.-H.; Wang, C.-H.; Shu, C.-F. *Inorg. Chem.* **2005**, *44*, 7770. (c) Chang, S.-Y.; Kavitha, J.; Li, S.-W.; Hsu, C.-S.; Chi, Y.; Yeh, Y.-S.; Chou, P.-T.; Lee, G.-H.; Carty, A. J.; Tao, Y.-T.; Chien, C.-H. *Inorg. Chem.* **2006**, *45*, 137. (d) Yang, C.-H.; Cheng, Y.-M.; Chi, Y.; Hsu, C.-J.; Fang, F.-C.; Wong, K.-T.; Chou, P.-T.; Chang, C.-H.; Tsai, M.-H.; Wu, C.-C. *Angew. Chem., Int. Ed.* **2007**, *46*, 2418.
(16) (a) Coppo, P.; Plummer, E. A.; De Cola, L. *Chem. Commun.* **2004**, 1774. (b) Orselli, E.; Kottas, G. S.; Konradsson, A. E.; Coppo, P.; Fröhlich, R.; De Cola, L.; van Dijken, A.; Büchel, M.; Börner, H. *Inorg. Chem.* **2007**, *46*, 11082.
(17) Stagni, S.; Orselli, E.; Palazzi, A.; De Cola, L.; Zacchini, S.; Femoni, C.; Marcaccio, M.; Paolucci, F.; Zanarini, S. *Inorg. Chem.* **2007**, *46*, 9126.
(18) (a) Chang, S.-Y.; Kavitha, J.; Hung, J.-Y.; Chi, Y.; Cheng, Y.-M.; Li, E. Y.; Chou, P.-T.; Lee, G.-H.; Carty, A. J. *Inorg. Chem.* **2007**, *46*, 7064. (b) Chang, S.-Y.; Chen, J.-L.; Chi, Y.; Cheng, Y.-M.; Lee, G.-H.; Jiang, C.-M.; Chou, P.-T. *Inorg. Chem.* **2007**, *46*, 11202.
(19) Nonoyama, M.; Takayanagi, H. *Transition Met. Chem.* **1976**, *1*, 10.
(20) Maestri, M.; Sandrini, D.; Von Zelewsky, A.; Deuschel-Cornioley, C. *Inorg. Chem.* **1991**, *30*, 2476.
(21) (a) Koo, C.-K.; Lam, B.; Leung, S.-K.; Lam, M.H.-W.; Wong, W.-Y. *J. Am. Chem. Soc.* **2006**, *128*, 16434. (b) Koo, C.-K.; Ho, Y.-M.; Chow, C.-F.; Lam, M.H.-W.; Lau, T.-C.; Wong, W.-Y. *Inorg. Chem.* **2007**, *46*, 3603.
(22) Willison, S. A.; Jude, H.; Antonelli, R. M.; Rennekamp, J. M.; Eckert, N. A.; Krause Bauer, J. A.; Connick, W. B. *Inorg. Chem.* **2004**, *43*, 2548.
(23) For a review, see: (a) Halcrow, M. A. *Coord. Chem. Rev.* **2005**, *249*, 2880.
(24) Willison, S. A.; Krause, J. A.; Connick, W. B. *Inorg. Chem.* **2008**, *47*, 1258.
(25) For a review, see: (a) Lindley, J. *Tetrahedron* **1984**, *40*, 1433.
(26) Goodbrand, H. B.; Hu, N.-X. *J. Org. Chem.* **1999**, *64*, 670.
(27) (a) Klapars, A.; Antilla, J. C.; Huang, X.; Buchwald, S. L. *J. Am. Chem. Soc.* **2001**, *123*, 7727. (b) Antilla, J. C.; Baskin, J. M.; Barder, T. E.; Buchwald, S. L. *J. Org. Chem.* **2004**, *69*, 5578.
(28) Klapars, A.; Buchwald, S. L. *J. Am. Chem. Soc.* **2002**, *124*, 14844.

Scheme 3. Structures of the Platinum(II) Complexes Reported

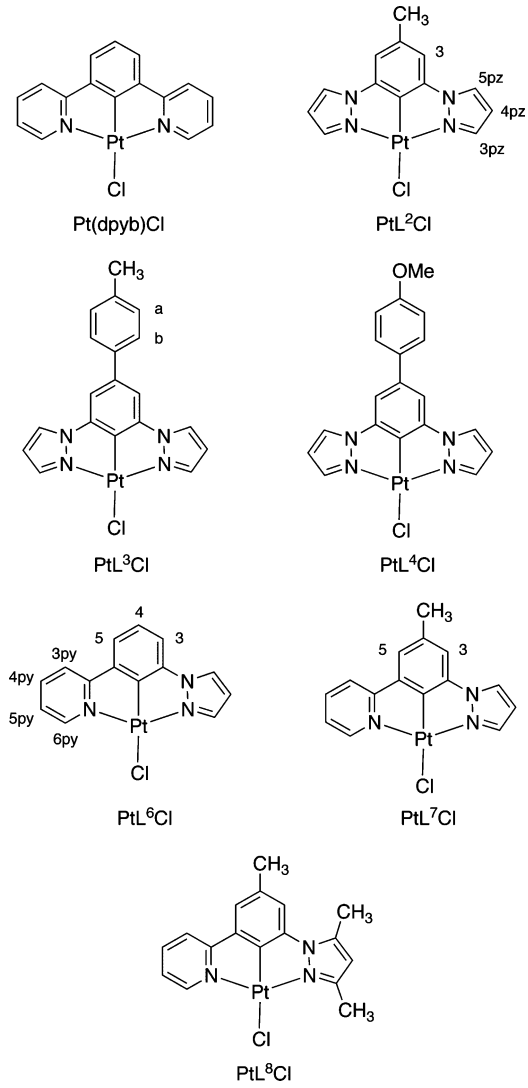

aromatic, we isolated a mixture of the desired compound 1,3-di-iodo-5-methyl-benzene, the singly reacted compound 1-iodo-3-bromo-5-methyl-benzene, and the starting material, in the mole ratio 47:41:12 by ^{1}H NMR after 3 days. This ratio was remarkably consistent between runs, and the proportion of starting material was not significantly increased by using longer reaction times (5 days) or by addition of fresh catalyst, suggesting that an equilibrium is reached. Subsequent copper-catalyzed reaction of the crude mixture with pyrazole led to a readily separable mixture of 1,3-bis(1-pyrazolyl)-5-methyl-benzene (HL^2) and 1-bromo-3-(1-pyrazolyl)-5-methyl-benzene, *pre-7* (Scheme 4,b).

The mixed py-pyz ligands HL^6 and HL^7 were obtained from the singly substituted side products *pre-6* and *pre-7* respectively, by means of a palladium-catalyzed Stille cross-coupling reaction with 2-tri(n-butyl)stannylpyridine, as used in the synthesis of dpybH and its derivatives.[11] The use of 3,5-dimethylpyrazole led to HL^8 in the same way.

The 5-aryl-substituted ligands HL^{3-5} were prepared in three steps from 1,3,5-tribromobenzene, tbb (Scheme 4,c). Palladium-catalyzed Suzuki cross-coupling of tbb with 1 equiv of the appropriate arylboronic acid, and chromatographic purification to remove undesired disubstituted material and unreacted tbb, was followed by copper-catalyzed halogen exchange and subsequent bis-amination with pyrazole as for HL^2.

The C-linked, 3-pyrazolyl isomer of HL^1, namely 1,3-di(3-pyrazolyl)benzene, HL^9, in which the pyrazole rings are connected to the central aryl ring via C^3 rather than N^1, was prepared from 1,3-diacetyl benzene by condensation of its bis(dimethylaminochalcone) derivative, *pre-9*, with hydrazine (Scheme 5).[29] Bis-N-arylation of HL^9 to generate derivatives HL^{10} and HL^{11} was accomplished under the same copper-catalyzed conditions as those used in the synthesis of HL^{2-7}.

Synthesis and Characterization of Platinum(II) Complexes. Attempts to prepare the N^C^N-coordinated platinum(II) complex of HL^1, PtL^1Cl, in acetic acid led to mixtures of products, only one of which were we able to isolate cleanly. The ^{1}H NMR of this compound confirmed that cyclometalation had occurred, but the symmetry of the ligand had been lost, with the two pyrazoles in different environments. We speculated that this might be due to the Pt(II) ion cyclometalating at position C^4 of the ligand rather than C^2: such competitive binding to give the kinetic product has been observed previously for dpyb with Pd(II)[30] and Ir(III).[31] We reasoned that it might be possible to inhibit such binding through the steric influence of a substituent introduced at position C^5 of the central aryl ring, and thus abandoned further studies with HL^1 in favor of C^5-substituted ligands. Meanwhile, Connick and co-workers had also been investigating the coordination chemistry of HL^1 with Pt(II) and, toward the end of our experimental work, they reported that the product formed from HL^1 and K_2PtCl_4 in acetic acid after long reaction times is, in fact, a trimer, $[Pt(\mu\text{-}L^1)Cl]_3$, the structure of which they confirmed conclusively by crystallography.[24] The ligand is metallated at position C^4 in an N^C fashion involving one of the two pyrazole rings, with the second pyz bound to a neighboring platinum(II) ion. They were also able to isolate the monomeric complex $[PtL^1Cl]$ that had eluded us, by using shorter reaction times and lower concentrations of platinum(II) salts.[24]

The strategy of introducing substituents at position C^5 of the ligand proved successful in directing metalation to C^2, even for the sterically undemanding methyl group. Thus, the reaction of HL^2 with K_2PtCl_4 in acetic acid led to precipitation of PtL^2Cl, analytically pure after a simple washing sequence. No evidence was found for the formation of C^4-metalated products. The aryl-substituted complexes PtL^3Cl and PtL^4Cl were obtained similarly, although the more electron-rich amino derivative HL^5 failed to provide a tractable complex. Similarly, HL^{2M} carrying methyl substituents in the pyrazole rings gave

(29) Pleier, A. K.; Glas, H.; Grosche, M.; Sirsch, P.; Thiel, W. R. *Synthesis* **2001**, *1*, 55.
(30) Cárdenas, D. J.; Echavarren, A. M.; Ramíre de Arellano, M. C. *Organometallics* **1999**, *18*, 3337.
(31) (a) Wilkinson, A. J.; Goeta, A.; Foster, C. E.; Williams, J. A. G. *Inorg. Chem.* **2004**, *43*, 6513. (b) Wilkinson, A. J.; Puschmann, H.; Howard, J. A. K.; Foster, C. E.; Williams, J. A. G. *Inorg. Chem.* **2006**, *45*, 8685.

Scheme 4. Synthetic Strategies Employed in the Preparation of the N-Linked Pyrazole-Containing Ligands HL^{2-8}

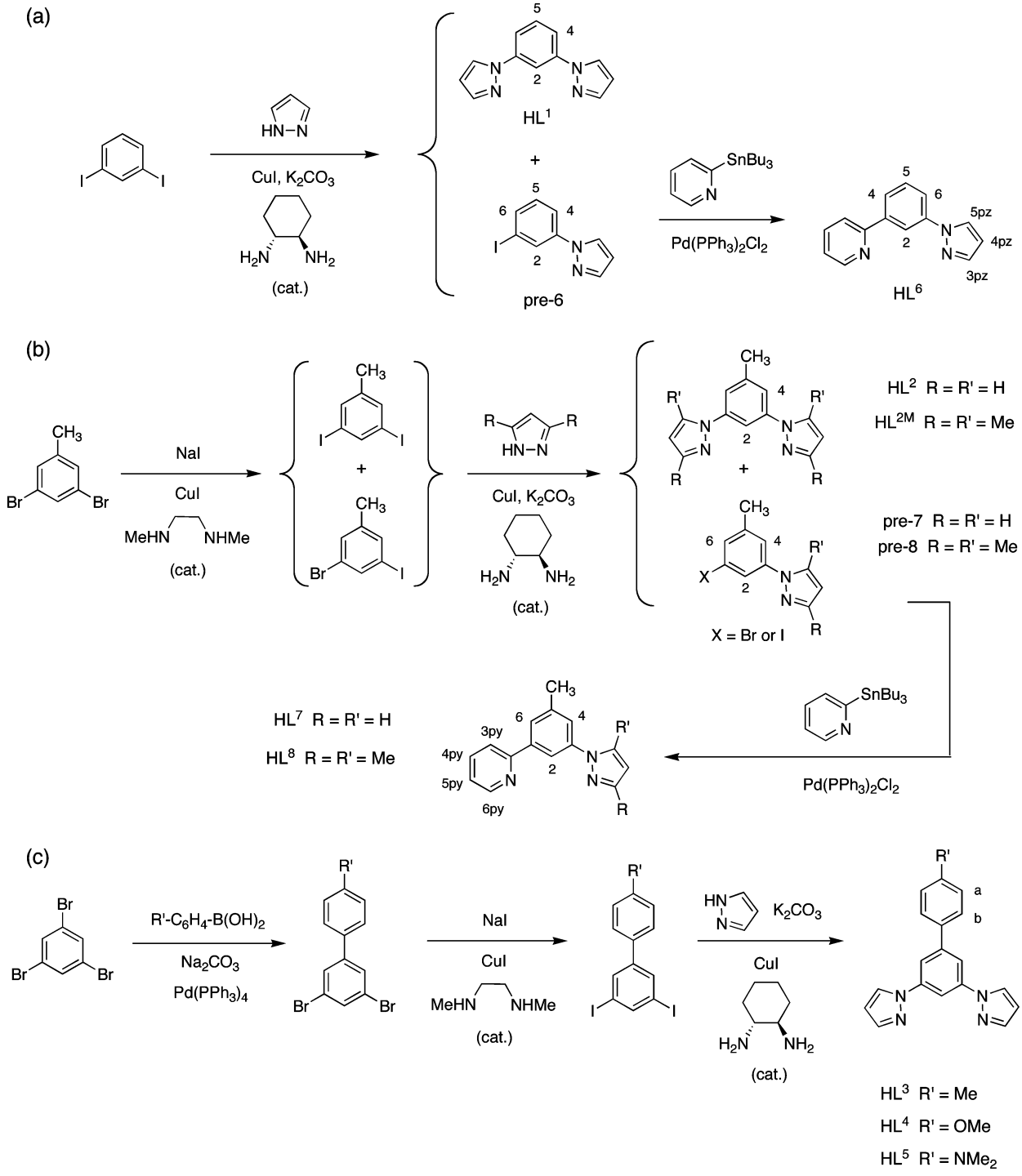

an unseparable mixture of products, perhaps associated with the lack of good π-accepting units within the ligand to satisfy the electron density at the metal.

Apart from the loss of the H^2 resonance (atom numbering system of Scheme 4), the main systematic changes in the ^{1}H NMR spectra of the ligands upon coordination to Pt(II) in a N^C^N manner were found to be as follows: (i) a shift in the H^3pz resonance to higher frequency ($\Delta\delta$ 0.3 ppm); (ii) a shift in the H^4 resonances to lower frequency ($\Delta\delta$ −0.6 ppm); and (iii) the appearance of ^{195}Pt ($I = 1/2$) satellites for H^3pz and H^5pz (coupling constants of the order of 13 Hz), H^4 (∼ 8 Hz) and H^4pz (not quantitatively resolvable at the field strengths employed but evident from the peak shape).

The Pt(II) complexes of the asymmetric py-pyz ligands, HL^{6-8}, were prepared in the same way. In this case, even the unsubstituted ligand HL^6 gave the N^C^2^N-coordinated product, with no evidence of competitive binding at C^4 or C^6. The changes in the ^{1}H NMR spectra for the two halves of the ligands were directly comparable to those observed in the respective bis-pyrazolyl and bis-pyridyl ligands. The value of $^3J(^{195}\text{Pt})$ is markedly larger for H^6py than for H^3pz

(~ 44 and 13 Hz respectively), in line with the smaller H−H coupling constants observed in pyrazole rings compared to pyridines.[32]

A crystal of complex PtL^7Cl, obtained by slow evaporation of an acetonitrile solution, was analyzed by X-ray diffraction, confirming the expected N^C^N-coordination (Figure 1). The Pt−C bond length of 1.917(7) Å is essentially identical to that found in the Pt(II) complexes of dipyridylbenzenes (average for 10 complexes for which data are available is 1.908 Å[9,11,30,33]) and also in Connick's N^C^N-coordinated bis-pyrazole complex PtL^1Cl {1.924(5) Å [24]}. As we have noted previously,[9] such values are significantly less than those of around 2.04 Å observed in N^N^C-coordinated complexes. The two Pt−N bond lengths are not significantly different from one another (values are given in the caption to Figure 1), and both they and the Pt−Cl are essentially identical to the values found in Pt(dpyb)Cl and derivatives,[9,11,30,33] and in PtL^1Cl.[24] The N−Pt−N angle of 160.7(2) is similar to that found in the dpyb complexes (which vary between 161.1(2) and 161.6(2) Å for the 10 complexes for which data are available), but larger than the value of 158.9(1)° for PtL^1Cl reported by Connick, who speculated that the strain associated with this rather small angle might account for the tendency of that complex to convert to the trimer.[24]

We also investigated the C-linked bis-pyrazole ligand, 1,3-di(3-pyrazolyl)benzene HL^9, an isomer of HL^1. A number of attempts to obtain the N^C^N-coordinated Pt(II) complex of this ligand (e.g., K_2PtCl_4 in CH_3CO_2H at reflux; $Pt(DMSO)_2Cl_2$ in MeOH at reflux) failed to give tractable products. Unlike HL^1, tautomerism in this ligand will lead to the co-existence of three different forms (N^1H/N^1H; N^1H/N^2H; N^2H/N^2H, cf. Scheme 2,a), which may potentially lead to more binding modes, perhaps again exacerbated by metalation at C^4/C^6. To block tautomerism and direct coordination to the desired N^2, we also prepared the N-arylated ligands HL^{10} and HL^{11}, but again, there was no evidence of formation of the N^C^N-coordinated complexes with Pt(II) by ^1H NMR spectroscopy. Mass spectrometry showed signals for HL^{10} bound as a unidentate ligand {e.g. $Pt(HL^9)(DMSO)Cl_2$}.

Electrochemistry of the Complexes. The complexes were investigated by cyclic voltammetry in acetonitrile solution, in the presence of Bu_4NBF_4 (0.1 M) as the supporting electrolyte; data are reported in Table 1 relative to ferrocene under the same conditions ($E^{ox}_{1/2} = 0.40$ V vs SCE[34]). The bis-pyrazole complexes $PtL^{2-4}Cl$ each display an irreversible reduction wave in the region between −2.5 and −2.8 V. The cathodic shift relative to Pt(dpyb)Cl and its derivatives, for which pseudo-reversible reduction occurs around −2.0 V, is consistent with the notion that reduction occurs on the heteroaromatic ring, and with the established view that pyrazole is a weaker π-acceptor than pyridine. Density-functional theory (DFT) calculations (see below) confirm that the LUMO is largely localized on the pyrazole ring, while a similar trend to more negative potentials was observed by Connick et al. in going from $[Pt(tpy)Cl]^+$ to $[Pt(bpp)Cl]^+$, {bpp is the bis(1-pyrazolyl) analogue of tpy)}.[22] The interpretation is further supported by the behavior of the mixed py-pyz complexes, $PtL^{6-8}Cl$, which display a pseudo-reversible wave between −2.3 and −2.4 V, attributable to reduction localized largely on the pyridyl ring, followed by an irreversible reduction around −2.9 V associated with the pyrazole.

Oxidations are irreversible for all of the compounds, as typically observed for platinum(II) complexes. The peak potential of the first oxidation wave of PtL^2Cl (0.35 V) is a little lower than that of Pt(dpyb)Cl (0.43 V), which would be consistent with a more electron-rich complex. The introduction of the tolyl substituent shifts the peak potential anodically to 0.56 V, while the methoxyphenyl-substituted complex lies between the two, at 0.43 V. The trend can perhaps be rationalized in terms of the opposing effects of σ-withdrawal and π-donation of aryl groups.[35] In terms of the σ-bonding framework, simple aryl substituents are electron-withdrawing relative to methyl, which would tend to lead to higher oxidation potentials for aryl derivatives, as observed. However, the effect can be partially offset by donation through the π-bonding framework, the influence of which will be increased by electron-donating substituents in the aryl ring; for example, the methoxy group in PtL^4Cl. The relative magnitudes of the σ-withdrawing and π-donating effects could then lead to the observed order in E_p^{ox}: $PtL^3Cl > PtL^4Cl > PtL^2Cl$.

Photophysical Properties. Absorption Properties. The bis-pyrazolyl complexes $PtL^{2-4}Cl$, which are off-white and scarcely colored to the eye, display strong absorption bands around 260 nm in dichloromethane solution at room temperature because of π-π^* transitions within the ligands (Table 1 and Figure 2). The extinction coefficients of these bands for the aryl-substituted complexes $PtL^{3-4}Cl$ are substantially increased compared to that of the methyl-substituted complex PtL^2Cl because of the more extended conjugation arising from the pendant ring. A set of bands observed at longer wavelengths in the region 315−370 nm, having no counterparts in the uncoordinated ligands, may reasonably be attributed to charge-transfer transitions that involve the metal, and/or the chloride co-ligand, and/or the cyclometalated aryl ring in which the electron density will be raised as compared to the free ligand. In fact, the bands in this region resemble in form those observed for Pt(dpyb)Cl and derivatives in the near-UV/visible region, but displaced toward the blue by about 50 nm (Figure 2). Such a displacement would be anticipated to arise for charge-transfer transitions that involve the pyrazole rings as acceptors, owing to the significantly poorer π-acceptor nature of pyrazole compared to pyridine.

(32) (a) Claramunt, R. M.; Sanz, D.; Santa María, M. D.; Jiménez, J. A.; Jimeno, M. L.; Elguero, J. *Heterocycles* **1998**, *47*, 301. (b) Echévarría, A.; Elguero, J.; Meutermans, W. *J. Heterocycl. Chem.* **1993**, *30*, 957.
(33) Rochester, D. L. Ph. D. Thesis, University of Durham, Durham, U.K., 2007.
(34) Connelly, N. G.; Geiger, W. E. *Chem. Rev.* **1996**, *96*, 877.
(35) Similar effects have been observed in 4′-aryl-substituted terpyridyl Pt(II) complexes and substituted bipyridyl Ru(II) complexes: (a) Michalec, J. F.; Bejune, S. A.; Cuttell, D. G.; Summerton, G. C.; Gertenbach, J. A.; Field, J. S.; Haines, R. J.; McMillin, D. R. *Inorg. Chem.* **2001**, *40*, 2193. (b) Damrauer, N. H.; Boussie, T. R.; Devenney, M.; McCusker, J. K. *J. Am. Chem. Soc.* **1997**, *119*, 8253.

Scheme 5. Synthesis of the C-Linked Pyrazolyl Ligands HL^{9-11}

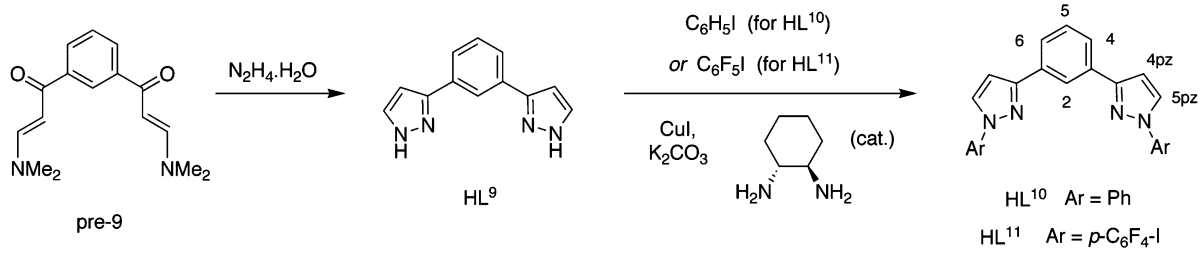

Table 1. Ground State UV-visible Absorption and Electrochemical Data of the Platinum Complexes in Solution at 298 K

complex	absorbance[a] λ_{max}/nm (ε/M^{-1} cm^{-1})	E_p^{ox}/V[b]	E_p^{red}/V [b] (ΔE /mV)
Pt(dpyb)Cl [c]	332 (6510), 380 (8690), 401 (7010), 454 (270), 485 (240)	0.43	−2.03
PtL^2Cl	246 (42000), 262 (38300), 284 (17100), 317 (7140), 326 (8340), 347 (5150), 360 (4750)	0.35	−2.76
PtL^3Cl	237 (27700), 266 (75800), 320 (8190), 329 (9390), 343 (7380), 365 (4460)	0.56	−2.50
PtL^4Cl	268 (70100), 285 (48900), 320 (9200), 330 (10700), 345 (8550), 369 (4510)	0.43	−2.65
PtL^6Cl	242 (39500), 265 (31400), 286 (21500), 298 (19100), 321 (6570), 356 (7220), 396 (2870), 446 (110), 478 (50)	0.26	−2.37 (90) −2.99
PtL^7Cl	242 (34600), 267 (23000), 299 (14700), 323 (5670), 345 (4190), 360 (5060), 405 (2240), 488 (35)	0.22	−2.36 (80) −2.89
PtL^8Cl	242 (28900), 266 (27000), 295 (15800), 317 (7770), 354 (5150), 400 (2170), 493 (30)	0.23	−2.39 (90) −2.93

[a] In solution in CH_2Cl_2. [b] In solution in MeCN, using Bu_4NPF_6 (0.1 M) as the supporting electrolyte. Peak potentials are given for the irreversible waves. For the pseudo-reversible reductions, values refer to $E_{1/2}$ and the peak-to-peak separation is given in parentheses. Values refer to a scan rate of 300 mV s^{-1} and are reported relative to $Fc^+|Fc$ ($E_{1/2}^{ox}$ = 0.40 V vs SCE). [c] Data from ref 11.

DFT calculations have been carried out for the complexes in the gas-phase using B3LYP (see Supporting Information): they strongly support this hypothesis. Thus, the electron density in the highest occupied molecular orbital (HOMO) is indeed seen to be localized predominantly on the metal, the chloride, and the central aryl ring of the terdentate ligand, while the LUMO is localized almost exclusively on the terdentate ligand, particularly on the pyrazole rings (Figure 3). Similar conclusions have been drawn previously for Pt(dpyb)Cl and simple derivatives, where the LUMO is localized on the pyridine rings[36] (frontier orbitals of other complexes are provided in the Supporting Information).

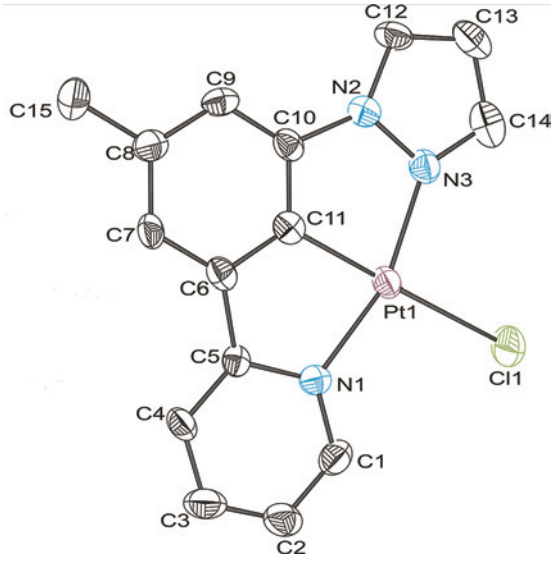

Figure 1. Asymmetric unit of PtL^7Cl in the crystal at 120 K, with the ellipsoids depicted at the 50% probability level. Hydrogen atoms and disorder of the L^7 ligand are omitted for clarity. Selected bond lengths (Å) and angles (deg): Pt(1)−C(11) 1.917(7), Pt(1)−N(1) 2.040(6), Pt(1)−N(3) 2.023(6), Pt(1)−Cl(1) 2.400(2); C(11)−Pt(1)−Cl(1) 178.5(2), N(1)−Pt(1)−N(3) 160.7(2), C(11)−Pt(1)−N(1) 80.1(3), C(11)−Pt(1)−N(3) 80.7(3).

In these bis-pyrazole complexes, there is no evidence of any lower energy bands arising from the direct S→T transition, in contrast to Pt(dpyb)Cl and derivatives, where weak bands ($\varepsilon \sim 200$) around 485 nm arise from direct excitation to the triplet state facilitated by spin-coupling associated with the platinum(II) ion.

The asymmetric py-pyz complexes, $PtL^{6-8}Cl$, display features of both the bis-pyrazole and bis-pyridyl complexes. Thus, they absorb out to longer wavelengths than $PtL^{2-4}Cl$, with maxima around 400 nm, comparable to Pt(dpyb)Cl albeit with lower extinction coefficients (Figure 4). In fact, there is qualitatively reasonable agreement between the absorption spectrum of the 4-methyl-substituted complex PtL^7Cl and that of the summation of the spectra of the

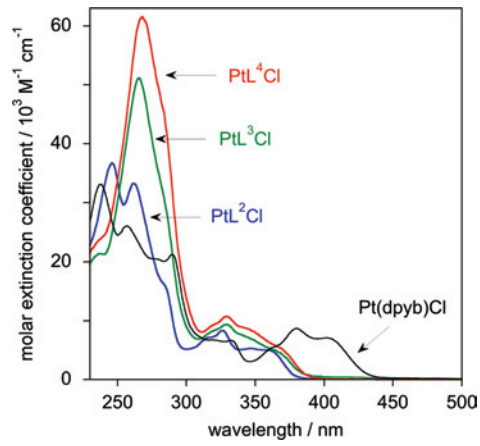

Figure 2. UV−visible absorption spectra of the bis-pyrazolyl complexes PtL^2Cl, PtL^3Cl, and PtL^4Cl in dichloromethane solution at 298 K, together with that of Pt(dpyb)Cl for comparison.

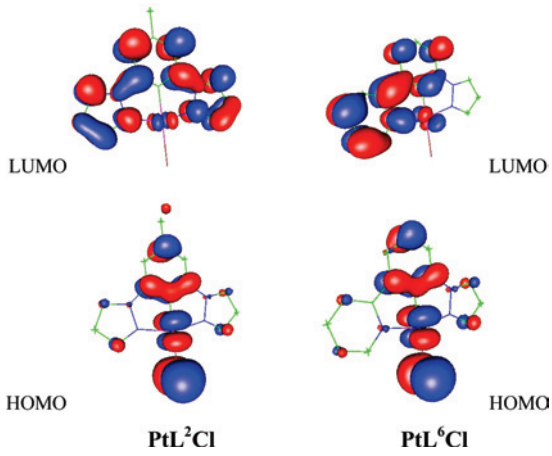

Figure 3. Frontier orbital plots of PtL^2Cl and PtL^6Cl obtained by DFT. Corresponding plots for the other complexes are provided in the Supporting Information.

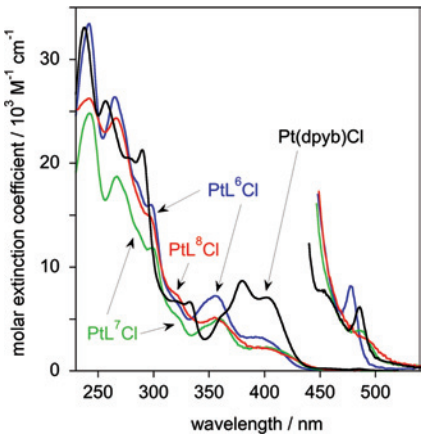

Figure 4. UV−visible absorption spectra of the asymmetric py-pyz complexes PtL^6Cl, PtL^7Cl, and PtL^8Cl, together with that of Pt(dpyb)Cl for comparison. The weak, low-energy bands around 480 nm are shown on an arbitrary expanded scale.

corresponding bis-pyrazole {PtL^2Cl} and bis-pyridyl {Pt(Me-dpyb)Cl} complexes, weighted 50% each (superimposed spectra are shown in the Supporting Information). That the lowest-energy spin-allowed absorption bands in these asymmetric complexes specifically involve the pyridyl groups is also supported by DFT calculations. They reveal that the LUMO is now asymmetrically distributed, being localized on the pyridyl ring, with essentially no contribution from the pyrazole (Figure 3). On the other hand, the HOMO again comprises significant contributions from the metal, the chloride co-ligand, and the metalated aryl ring.

The asymmetric complexes also display weak bands around 480 nm ($\varepsilon \sim 50$), sharp and well-resolved for PtL^6Cl but less so for the methyl-substituted complexes PtL^7Cl and PtL^8Cl, attributable to the S→T excitation as seen in the bis-pyridyl systems (Figure 4, expansion).[9]

Emission Properties. All of the new complexes reported here are luminescent in dichloromethane solution at room temperature. Data are summarized in Table 2.

(i) Bis-pyrazole Complex PtL^2Cl. The methyl-substituted bis-pyrazole complex PtL^2Cl displays a highly vibrationally structured emission spectrum, similar in profile to that of Pt(dpyb)Cl, but shifted substantially to the blue by almost 40 nm; $\lambda_{max} = 453$ nm (Figure 5). The change from pyridine to pyrazole rings increases the triplet excited-state energy by 1700 cm^{-1}. The result vindicates the proposition at the outset that the poorer π-acceptor character of pyrazole compared to pyridine should lead to an increase in the energy of the LUMO and hence of the excited state. Somewhat related results have been observed in the chemistry of Pt(II) and Ir(III) with bidentate ligands, where some of the most blue-emitting complexes are those which incorporate azole rings.[15,16,18] We also note that the complex is only weakly solvatochromic (overlaid spectra in different solvents are provided in the Supporting Information). This would be consistent with the qualitative picture from the frontier orbitals of a symmetrical redistribution of the electron density "outwards" from the principal axis of the molecule, which would have only a relatively small influence on the dipole moment.

The higher energy of the emission relative to the bis-pyridyl complexes is accompanied by a reduction in the luminescence quantum yield: $\Phi_{lum} = 0.02$ compared to 0.60 for Pt(dpyb)Cl. Some insight into the origin of this decrease in efficiency can be obtained from the radiative and non-radiative rate constants, which may be estimated from the measured values of quantum yield and lifetime ($\tau = 4.0$ μs at infinite dilution) if it is assumed that the emissive excited state is formed with unitary efficiency upon excitation. This analysis reveals that the inferior quantum yield is the combined result of a substantially lower radiative rate constant {$k_r = 5000$ s^{-1} for PtL^2Cl compared to 83000 s^{-1} for Pt(dpyb)Cl} and increased rate of non-radiative decay {k_{nr} values are 25×10^4 and 5.6×10^4 s^{-1}, respectively} (Table 2). The lower radiative rate constant could be accounted for in terms of a lower contribution of metal character to the excited state, in line with the more electron-rich nature of the pyrazole ligand system which will lead to more ligand-centered character. The greater susceptibility of the excited state to non-radiative decay may be associated, in part, with the N^C^N-coordination in the bis-pyrazole system being less rigid than in the bis-pyridines because of the less appropriate bite angle, and thus to distortion of the molecule upon formation of the excited state. This notion is supported by two experimental observations: (i) the relative intensities of the $v'' = 1$ and $v'' = 2$ vibrational bands to the $v'' = 0$ in PtL^2Cl are higher than in Pt(dpyb)Cl, consistent with a greater displacement of the excited-state potential energy surface relative to the ground state; and (ii) there is a pronounced blue-shift of 1200 cm^{-1}, and an increase in the lifetime by a factor of 3, upon going from room temperature solution to a rigid glass at 77 K (Figure 6), whereas the spectra and lifetimes of the bis-pyridyl series of complexes are essentially unaffected by temperature.[11] It is also possible that the higher energy of the excited state brings it sufficiently close to higher-lying metal-centered states to open up thermally activated population of such states as a decay pathway.[37]

Only at low concentrations ($<5 \times 10^{-6}$ M) is the well-defined, structured emission spectrum of Figure 5 observed for PtL^2Cl. As the concentration increases, a broad band

Table 2. Luminescence Data for the Platinum Complexes in CH_2Cl_2 Solution at 298 K except Where Stated Otherwise

								emission at 77 K[g]	
complex	emission[a] λ_{max}/nm	Φ_{lum}[b]	$\tau_0/\mu s$[c,d] degassed (aerated)	k_Q^{SQ} / 10^8 M^{-1} s^{-1}[c]	k_r / 10^3 s^{-1} [e]	$\sum k_{nr}$ / 10^4 s^{-1} [e]	k_Q^{O2} / 10^8 M^{-1} s^{-1} [f]	λ_{max}/nm	$\tau/\mu s$
Pt(dpyb)Cl	491, 524, 562 excimer: 695	0.60	7.2 (0.5)	53	83	5.6	8.5	487, 521, 558	6.1
PtL^2Cl	453, 482, 514, aggregate: 555	0.02	4.0 (0.24)	23	5.0	25	1.8	430, 460, 489	11
PtL^3Cl	491, 520	0.15	21 (0.10)	4.0	7.1	4.1	45	480, 512, 548	39
PtL^4Cl	507, 535	0.12	22 (0.12)	5.7	5.5	4.0	38	482, 515, 552	41
PtL^6Cl	487, 522, 560, excimer: 645	0.64	6.9 (0.55)	6.6	93	5.2	7.6	480, 517, 551, 594(sh)	8.8
PtL^7Cl	503, 537, 577(sh)	0.53	10.0 (0.43)	6.5	53	4.7	10	494, 531, 567, 614	10.5
PtL^8Cl	509, 541, 587(sh)	0.32	8.8 (0.29)	2.0	36	7.8	15	498, 536, 573, 623	9.7

[a] Emission maxima following excitation into the lowest-energy spin-allowed absorption band. [b] Luminescence quantum yield measured using quinine sulfate in 1 M H_2SO_4 *(aq)* as the standard. [c] τ_0 is the lifetime at infinite dilution and k_Q^{SQ} the bimolecular self-quenching rate constant, determined from the *y*-intercept and gradient, respectively, of a plot of τ^{-1} versus concentration. [d] $\lambda_{ex} = 374$ nm. [e] Radiative (k_r) and non-radiative ($\sum k_{nr}$) rate constants calculated from τ and ϕ values at 298 K. [f] Bimolecular rate constant for quenching by O_2, estimated from τ values in degassed and aerated solutions. [g] In diethyl ether−isopentane−ethanol, 2:2:1 by volume.

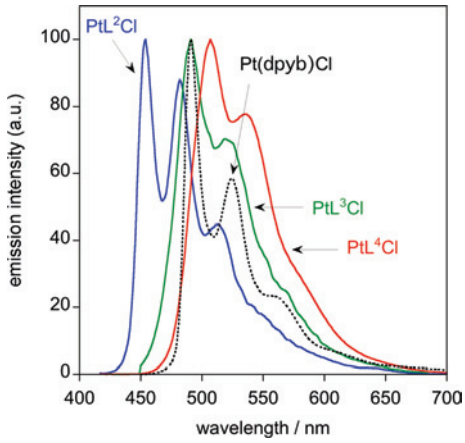

Figure 5. Emission spectra of the bis-pyrazole complexes $PtL^{2-4}Cl$ in dilute solution in degassed dichloromethane (2×10^{-6} M) at 298 K ($\lambda_{ex} = 360$ nm, band-passes of 2.0 nm). The dotted line shows the emission spectrum of Pt(dpyb)Cl under the same conditions for comparison.

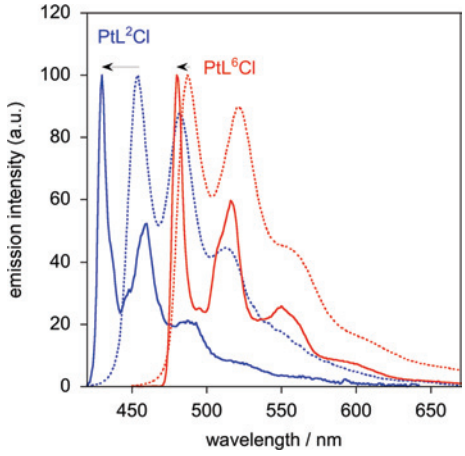

Figure 6. Solid lines: Emission spectra of PtL^2Cl (blue) and PtL^6Cl (red) at 77 K in a glass of diethyl ether−isopentane−ethanol (2:2:1 by volume). Dotted lines: the corresponding spectra in CH_2Cl_2 at 298 K for comparison. The arrows highlight the direction and magnitude of the blue-shifts upon cooling.

centered around 555 nm begins to appear (Figure 7). The lifetime (τ_{obs}) of the 453 nm band decreases concomitantly, initially following a Stern−Volmer type equation of the form $\tau_{obs} = \tau_0 + k_Q^{SQ}$ [Pt] (where τ_0 is the emission rate constant at infinite dilution and k_Q^{SQ} is the apparent rate constant of self-quenching) but, at higher concentrations, the emission decay ceases to be exponential. In the Pt(dpyb)Cl series, the

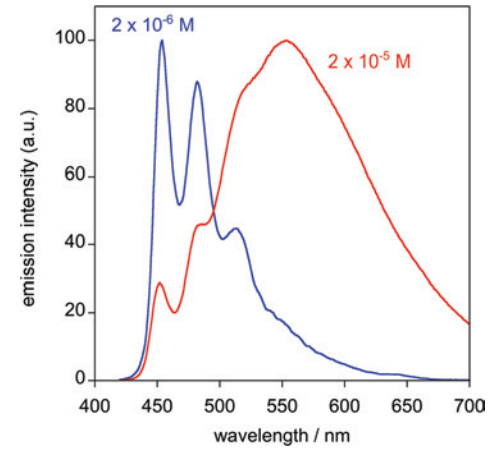

Figure 7. Concentration dependence of the emission spectrum of PtL^2Cl in CH_2Cl_2 at 298 K: spectra at 2×10^{-6} M (blue) and 2×10^{-5} M (red) showing the appearance of an additional new band at low energy.

appearance of a low energy band around 700 nm has been attributed to the formation of an excimer, formed by the diffusion-controlled encounter of an excited-state complex with the complex in its ground state. In the present case of PtL^2Cl, at least two experimental observations suggest that the process involves a ground-state interaction of the molecules rather than an excimer. First, the profile of the excitation spectrum begins to deviate from that of the absorption spectrum, even at concentrations where the optical density is sufficiently low for inner-filter effects to be minimal. This suggests a change in speciation in solution. Second, the grow-in of the new, low-energy emission was too fast to be resolved on the nanosecond time scale (using equipment with a response function ~ 0.5 ns). This contrasts with the excimer emission displayed by Pt(dpyb)Cl, whose growth is characterized by a much slower time-constant of the order of 1 μs, reflecting the diffusion-controlled nature of excimer formation. These observations imply that the species responsible for the lower-energy band in PtL^2Cl is already present in solution prior to excitation, presumably through ground-state aggregation. It is also noteworthy that in the solid state (powder), PtL^2Cl displays bright green photoluminescence with an emission maximum around 530 nm, very different from that of the dilute solution, and again suggesting the influence of ground-state intermolecular interactions on the excited-state properties of this compound.

(ii) Aryl-Substituted Bis-pyrazole Complexes PtL$^{3-4}$Cl. The 4-aryl-substituted complexes, PtL^{3}Cl and PtL^{4}Cl, display emission spectra that are red-shifted relative to that of PtL^{2}Cl by approximately 40 and 50 nm respectively (in CH_2Cl_2 solution at room temperature; Figure 5). The trend of decreasing excited-state energies on going from PtL^{2}Cl through PtL^{3}Cl to PtL^{4}Cl can be attributed to the influence of the pendant aryl groups in extending the conjugation, through their π-donating and σ-withdrawing nature which can serve to raise the HOMO and lower the LUMO respectively; such an effect, predominantly via the HOMO, has been observed previously for the 4-aryl-substituted derivatives of Pt(dpyb)Cl, where the emission energy decreased as a function of the electron-donating power of the substituent.[11] Although the spectra display clear vibrational structure, with the 0−0 band again being the most intense, the structure is somewhat less well-defined than for PtL^{2}Cl, and the constituent bands are broader. This difference in profile probably arises from the thermal distribution of conformers having different torsion angles between the N^C^N framework and the aryl pendant, each with slightly different excited-state energies. For example, a similar trend has been observed in the π-π* states of terpyridyl iridium(III) complexes upon aryl substitution.[38]

At 77 K in an EPA glass, the spectra of PtL^{3}Cl and PtL^{4}Cl both shift to the blue, but the shift is larger for the latter, such that the two compounds have essentially identical spectra under these conditions (Figure 8). The torsional rearrangement necessary to bring the pendant aryl group from the preferred geometry in the ground state (typical dihedral angles for biaryls are 30° or more) to the conformation required to maximize the conjugation in the excited state (approximately coplanar with the N^C^N plane), will be inhibited in the rigid glass, leading to the similar behavior for both complexes.

The luminescence lifetimes of PtL$^{3-4}$Cl are long, around 20 μs in degassed CH_2Cl_2 at 298 K (Table 2), compared to 4 μs for PtL^{2}Cl under the same conditions. The quantum yields are also superior to that of PtL^{2}Cl by almost an order of magnitude (Table 2). The data suggest that the improvement stems from a reduction in the non-radiative decay, $\sum k_{nr}$, whereas the radiative rate constant, k_r, is not significantly affected. At 77 K, the lifetimes increase to 40 μs. Such values are an order of magnitude longer than those of the archetypal MLCT emitters {e.g. for $[Ru(bpy)_3]^{2+}$, $\tau = 3.8$ μs at 77 K[39]}, and the k_r values at least an order of magnitude smaller, in line with the notion that a more predominantly ligand-centered description of the excited state is appropriate.

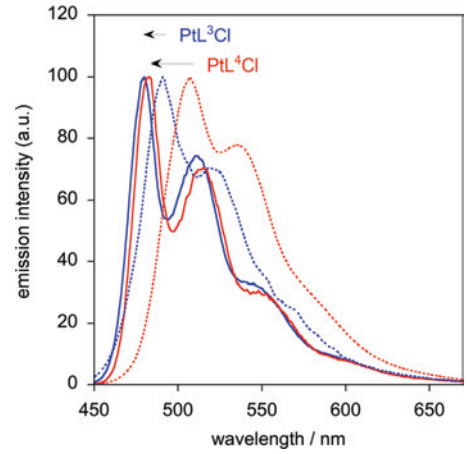

Figure 8. Solid lines: Emission spectra of PtL^{3}Cl (blue) and PtL^{4}Cl (red) at 77 K in a glass of diethyl ether−isopentane−ethanol (2:2:1 by volume). Dotted lines: the corresponding spectra in CH_2Cl_2 at 298K for comparison. The arrows highlight the direction and magnitude of the blue-shifts upon cooling.

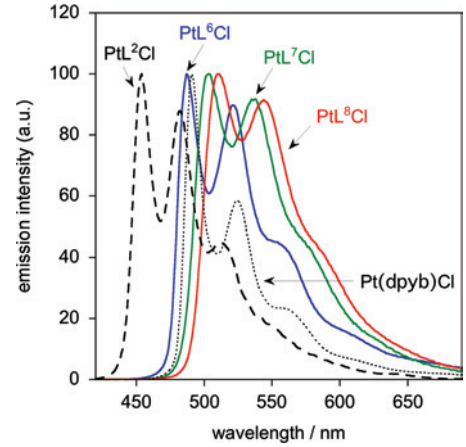

Figure 9. Emission spectra of the py-pyz complexes PtL^{6}Cl (blue), PtL^{7}Cl (green), and PtL^{8}Cl (red) in dilute solution in degassed dichloromethane (10^{-5} M) at 298 K ($\lambda_{ex} = 400$ nm, band-passes of 2.0 nm). The dotted and dashed lines are the emission spectra of Pt(dpyb)Cl and PtL^{2}Cl under the same conditions for comparison.

The aryl-substituted complexes are less sensitive to self-quenching at elevated concentrations than PtL^{2}Cl (k_Q^{SQ} are given in Table 2). This lower propensity to quenching is likely to arise from the additional steric hindrance to bimolecular interactions arising from the pendant aryl group, an effect that has also been observed in the aryl-substituted derivatives of Pt(dpyb)Cl.[11] Unlike PtL^{2}Cl, there is no change in the emission profile at high concentrations, suggesting either that aggregates or excimers do not form in this case or that they are non-emissive.

(iii) Asymmetric Pyridyl-Pyrazole Complexes PtL$^{6-8}$Cl. The emission spectra of the mixed py-pyz complexes PtL$^{6-8}$Cl in dilute solution are similar to that of Pt(dpyb)Cl (Figure 9). The emission maxima of the unsubstituted complex PtL^{6}Cl are almost identical to those of Pt(dpyb)Cl, and the luminescence quantum yields (0.64 and 0.60) and lifetimes (6.9 and 7.2 μs, Table 2) of the two complexes are the same within the uncertainty of the measurements. This

(36) Sotoyama, W.; Satoh, T.; Sato, H.; Matsuura, A.; Sawatari, N. *J. Phys. Chem. A* **2005**, *109*, 9760.
(37) Note added prior to publication: While this manuscript was under review, Haga et al. reported on iridium(III) complexes with closely related 1,3-bis(3-methylpyrazole)aryl ligands. The very low emission quantum yields of these complexes was shown to be due to the presence of a low-lying d-d state, through which thermally-activated non-radiative decay can occur. Yang, L.; Okuda, F.; Kobayashi, K.; Nozaki, K.; Tanabe, Y.; Ishii, Y.; Haga, M. *Inorg. Chem.* **2008**, *47*, 7154.
(38) (a) Collin, J.-P.; Dixon, I. M.; Sauvage, J.-P.; Williams, J. A. G.; Barigelletti, F.; Flamigni, L. *J. Am. Chem. Soc.* **1999**, *121*, 5009. (b) Goodall, W.; Batsanov, A. S.; Howard, J. A. K.; Williams, J. A. G. *Dalton Trans.* **2004**, 623. (c) Williams, J. A. G.; Wilkinson, A. J.; Whittle, V. L. *Dalton Trans.* **2008**, 2081.
(39) Lytle, F. E.; Hercules, D. M. *J. Am. Chem. Soc.* **1969**, *91*, 253.

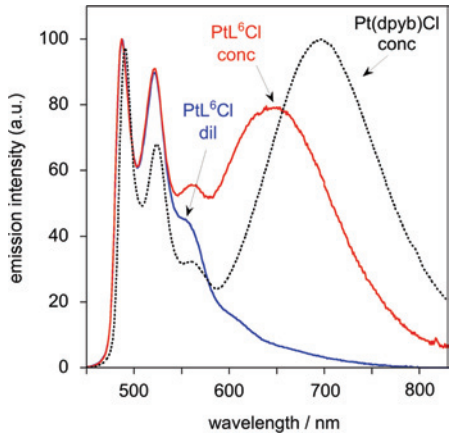

Figure 10. Influence of concentration on the emission spectrum of PtL^6Cl. Spectra in degassed CH_2Cl_2 at 10^{-5} M (blue), showing exclusively monomer emission, and at 3×10^{-4} M (red), in which the monomer is accompanied by an excimer band centered at 650 nm. The spectrum of a concentrated solution of Pt(dpyb)Cl is also shown for comparison of the excimer energies.

close similarity is consistent with the notion that the frontier orbitals in these complexes have essentially no contribution from the pyrazole ring, the LUMO being largely localized on the pyridine ring and the HOMO involving primarily the central aryl ring, the metal and the chloride ligand, as discussed earlier. The degree of solvatochromism is again minimal (plots are provided in the Supporting Information). The introduction of a methyl group at position 4 of the cyclometallating ring (PtL^7Cl) red-shifts the emission by 16 nm, similar to the effect in the corresponding derivative of Pt(dpyb)Cl, while a further small shift of 6 nm arises in PtL^8Cl from the methyl groups in the pyrazole ring.

Despite the close similarity between the emission of $PtL^{6-8}Cl$ and Pt(dpyb)Cl in dilute solution, the presence of the pyrazole does exert an influence on the behavior at higher concentrations. From the k_Q^{SQ} values, the propensity for self-quenching is reduced by almost an order of magnitude (Table 2). In the case of the unsubstituted complex, PtL^6Cl, an excimer band is observed, but which is dramatically blue-shifted compared with that displayed by Pt(dpyb)Cl (Figure 10). Evidently, the presence of the electron-rich pyrazole ring destabilizes the excimer, despite having no significant effect on the monomeric excited state. Excimer formation involves an electron donor−acceptor interaction between excited and ground-state molecules, and the increased electron density in the pyrazole ring presumably makes the ground state a poorer π-acceptor in its interactions with the excited-state molecule. Consistent with this explanation is the observation that the most electron-rich, dimethyl-pyrazolyl system, PtL^8Cl, is the least sensitive complex to self-quenching, based on the magnitude of k_Q^{SQ} (Table 2). The result contrasts with the previously observed *insensitivity* of the excimer energy in the Pt(dpyb)Cl-based systems to substituents at the 4-position of the cyclometallating ring. No excimer band could be detected in the case of PtL^7Cl or PtL^8Cl, highlighting the subtlety of the intermolecular interactions in these systems.

Conclusions

In summary, the copper-diamine catalyzed, Buchwald-type cross-coupling of pyrazoles with di-iodo aromatics provides access to potentially N^C^N-coordinating 1,3-bis(1-pyrazolyl)benzenes under mild conditions. Dibromoaromatics may be employed, preferably if they are first subjected to bromo-iodo exchange, which can be accomplished under similarly mild copper catalysis. Mixed pyridyl-pyrazole ligands are also accessible by reaction of the monopyrazole-substituted side products with 2-pyridylstannanes.

Cyclometalation of platinum(II) to 1,3-bis(1-pyrazolyl)-benzenes can be directed toward the C^2 position of the ligand, leading exclusively to N^C^N-coordinated complexes, by the presence of methyl or aryl substituents at C^5, which inhibits competitive metalation at the adjacent C^4 position. No such competition is observed in the case of the mixed ligand 1-(1-pyrazolyl)-3-(pyridyl)benzene.

Several features of interest distinguish the emission properties of these complexes from those of structurally related dipyridylbenzenes. First, the poorer π-acceptor nature of the pyrazole compared to pyridine ring shifts the LUMO in the complex PtL^2Cl to higher energy compared to Pt(dpyb)Cl, leading to emission in the blue region. Blue triplet emitters remain an important target in the development of phosphorescent OLEDs. Second, aryl substituents at the central 4-position of the aryl ring counteract this effect in the excited state, but not in the ground state: the emission is red-shifted whereas the absorption is scarcely affected. These complexes are also much less sensitive to concentration-induced self-quenching. Third, while the complexes of the mixed ligands seem at first sight to behave much like Pt(dpyb)Cl in dilute solution, the presence of the pyrazole ring exerts a significant effect on the intermolecular interactions. Thus, the excimeric excited state in PtL^6Cl is significantly destabilized. Inspection of the resulting spectrum indicates broad and relatively uniform coverage over the range from 480 to 700 nm, of potential interest for the generation of white light. It contrasts with Pt(dpyb)Cl, for which emission in the 550−600 nm region is minimal, and where significant energy is lost in the near-IR region.

Experimental Section

^1H and ^{13}C NMR spectra, including NOESY and COSY, were recorded on a Varian 200, 300, or 500 MHz instruments. Chemical shifts (δ) are in ppm, referenced to residual protio-solvent resonances, and coupling constants are in Hertz. Electrospray ionization mass spectra were acquired on a time-of-flight Micromass LCT spectrometer; electron ionization (EI) and chemical ionization (CI) spectra were recorded at the EPSRC National Mass Spectrometry Service Centre. All solvents used in preparative work were at least Analar grade, and water was purified using the Purite system. Solvents used for optical spectroscopy were HPLC grade.

1,3-Bis(1-pyrazolyl)benzene HL[1]. A mixture of di-iodobenzene (500 mg, 1.5 mmol), pyrazole (310 mg, 4.5 mmol), potassium carbonate (1.25 g, 9.0 mmol), copper(I) iodide (11 mg, 60 μmol), and *trans*-1,2-diaminocyclohexane (68 mg, 0.6 mmol) in dioxane (5 mL) was degassed, and then heated at reflux with vigorous stirring under a nitrogen atmosphere for 24 h. After cooling to room temperature, the solution was filtered and the solvent was removed

from the filtrate under reduced pressure. The residue was purified by chromatography on silica gel using a gradient elution. The monoaminated compound 1-iodo-3-(1-pyrazolyl)-benzene (*pre-6*) eluted first at 80% hexane/20% diethyl ether, followed by HL[1], a pale yellow oil, at 55% hexane/45% diethyl ether (255 mg, 81%). Data for ***pre-6***: ^{1}H NMR ($CDCl_3$, 200 MHz): δ 8.07 (1H, t, ^4J = 2.0, H^2), 7.85 (1H, d, ^3J = 2.5, H^5pz), 7.70 (1H, d, ^3J = 1.5, H^3pz), 7.60 (2H, overlapping m, H^4 and H^6), 7.12 (1H, t, ^3J = 8.0, H^5), 6.43 (1H, dd, ^3J = 2.5, ^3J = 2.0, H^4pz). MS (ES+): *m/z* 271.0 (M + H^+). Data for **HL**[1]: ^{1}H NMR ($CDCl_3$, 500 MHz): δ 8.12 (1H, t, ^4J 2.0, H^2), 8.03 (2H, d, ^3J = 2.5, H^5pz), 7.76 (2H, d, ^3J = 1.5, H^3pz), 7.65 (2H, dd, ^3J = 8.0, ^4J = 2.0, H^4), 7.54 (1H, t, ^3J = 8.0, H^5), 6.51 (2H, m, H^4pz). ^{13}C NMR ($CDCl_3$, 500 MHz): 141.7 (C^3pz), 141.4 (C^1), 130.7 (C^5), 127.2 (C^5pz), 116.8 (C^4), 110.2 (C^2), 108.3 (C^4pz). MS (EI^+): *m/z* 210 (M^+).

1,3-Bis(1-pyrazolyl)-5-methyl-benzene HL[2]. Step 1. A mixture of 1,3-dibromo-5-methyl-benzene (680 mg, 2.7 mmol), sodium iodide (1.6 g, 10.9 mmol), copper(I) iodide (52 mg, 0.27 mmol), and *N*,*N*′-dimethylethylenediamine (48 mg, 0.54 mmol) in toluene (3 mL) was degassed, and then heated at reflux with vigorous stirring for 48 h. After cooling, the solvent was removed under reduced pressure, and the residue was taken up into a mixture of dichloromethane (50 mL) and aqueous sodium hydroxide (1 M, 30 mL). The organic phase was separated, washed with water, dried over anhydrous $MgSO_4$, and evaporated to dryness, to give a mixture of 1,3-di-iodo-5-methylbenzene, 1-iodo-3-bromo-5-methylbenzene, and the starting material dibromotoluene. The compounds are not readily separable by chromatography: it proves more straighforward to use the crude mixture directly in Step 2. ^{1}H NMR for the di-iodo product ($CDCl_3$, 300 MHz): δ 7.85 (1H, s, H^2), 7.48 (2H, s, H^4), 2.25 (3H, s, CH_3).

Step 2. The crude mixture from Step 1 was subject to the copper-catalyzed amination with pyrazole, as described for HL[1]. After workup, the crude mixture was purified by column chromatography on silica using a gradient elution. The side product 1-bromo-3-(1-pyrazolyl)-5-methyl-benzene (*pre-7*) eluted first at 80% hexane/20% diethyl ether, followed by 1,3-bis(1-pyrazolyl)-5-methyl-benzene, HL[2] at 60% hexane/40% diethyl ether (80%). Data for ***pre-7***: ^{1}H NMR ($CDCl_3$, 300 MHz): δ 7.89 (1H, d, ^3J = 2.5, H^5pz), 7.71 (1H, d, ^3J = 1.5, H^3pz), 7.67, 7.48, 7.24 (each 1H, s, H^2, H^4 and H^6), 6.47 (1H, m, H^4pz), 2.39 (3H, s, CH_3). ES (MS^+) 237/239 (M + H^+ $^{79/81}$Br). Data for **HL**[2]: ^{1}H NMR ($CDCl_3$, 300 MHz): δ 7.99 (2H, d,^3J = 2.5, H^5pz), 7.85 (1H, t, ^4J = 2.0, H^2), 7.73 (2H, d, ^3J = 1.5, H^3pz), 7.46 (2H, t, ^4J = 2.0, H^4), 6.48 (2H, m, H^4pz), 2.47 (3H, s, CH_3). MS (ES^+): *m/z* 225 (M + H^+), 247 (M + Na^+). ^{13}C NMR ($CDCl_3$, 126 MHz): δ 141.5 (C^3pz), 141.2 (C^q), 141.1 (C^q), 127.2 (C^5pz), 117.7 (C^4), 108.1 (C^4pz), 107.4 (C^2), 21.9 (CH_3). Anal. Calcd for $C_{13}H_{12}N_4$: C, 69.6; H, 5.5; N, 25.0%. Found: C, 69.6; H, 5.4; N, 25.0%.

Data for ***pre-8*** and **HL^{2M}**, the 3,5-dimethylpyrazolyl analogues of *pre-7* and HL[2], are provided in the Supporting Information.

1,3-Bis(1-pyrazolyl)-5-p-substituted-aryl-benzenes HL[3]−HL[5]. Step 1. The preparation of the 1,3-dibromo-5-aryl-benzenes was accomplished by cross-coupling with the appropriate aryl boronic acid using the procedure described previously.[11]

Step 2. The 1,3-dibromo-5-aryl-benzene was subject to copper-catalyzed bromo-iodo exchange using the procedure described above for the synthesis of HL[2], step 1. The crude product, consisting primarily of the di-iodinated aromatic, was used directly in the next step without purification at this stage.

Step 3. The crude 1,3-di-iodo-5-aryl-benzene was subject to copper-catalyzed amination with pyrazole using the procedure described above for step 2 of the synthesis of HL[2].

HL[3]. From 1,3-dibromo-5-(4-methoxyphenyl)-benzene (240 mg, 0.74 mmol), giving HL[4] (55 mg, 25% over two steps), eluting at 70% hexane/30% diethyl ether. ^{1}H NMR ($CDCl_3$, 200 MHz): δ 8.07 (2H, d, ^3J = 2.5, H^5pz), 8.02 (1H, t, ^4J = 2.0, H^2), 7.84 (2H, d, ^4J = 2.0, H^4), 7.77 (2H, d, ^3J = 1.5, H^3pz), 7.60 (2H, d, ^3J = 8.0, H^b), 7.29 (2H, d, ^3J = 8.0, H^a), 6.52 (2H, dd, ^3J = 2.5, 1.5, H^4pz), 2.42 (3H, s, CH_3). MS (ES^+): *m/z* 301 (M + H^+).

HL[4]. From 1,3-dibromo-5-(4-methoxyphenyl)-benzene (300 mg, 0.88 mmol), giving HL[4] (48 mg, 15% over two steps), eluting at 70% hexane/30% diethyl ether. ^{1}H NMR ($CDCl_3$, 300 MHz): δ 8.04 (2H, d, ^3J = 2.5, H^5pz), 7.97 (1H, t, ^4J = 2.0, H^2), 7.80 (2H, d, ^4J = 2.0, H^4), 7.76 (2H, d, ^3J = 1.5, H^3pz), 7.61 (2H, d, ^3J = 9.0, H^b), 6.98 (2H, d, ^3J = 9.0, H^a), 6.52 (2H, appears as t, ^3J = 2.0, H^4pz), 3.84 (3H, s, CH_3). MS (ES^+): *m/z* 317 (M + H^+).

HL[5]. From 1,3-dibromo-5-(4-(dimethylamino)phenyl)-benzene (255 mg, 0.72 mmol), giving HL[5] (33 mg, 14% over two steps), eluting at 60% hexane/40% diethylether. ^{1}H NMR ($CDCl_3$, 200 MHz): δ 8.06 (2H, d, ^3J = 2.5, H^5pz), 7.94 (1H, t, ^4J = 2.0, H^2), 7.83 (2H, d, ^4J = 2.0, H^4), 7.77 (2H, d, ^3J = 1.5, H^3pz), 7.62 (2H, d, ^3J = 9.0, H^b), 6.81 (2H, d, ^3J = 9.0, H^a), 6.52 (2H, appears as t,^3J = 2.0, H^4pz), 3.03 (6H, s, NMe_2). MS (ES^+): *m/z* 330 (M+H^+).

Mixed Pyridyl-Pyrazole Ligands HL[6−8]. HL[6]. The precursor 1-bromo-3-(1-pyrazolyl)-benzene, *pre-6*, (130 mg, 0.48 mmol), 2-tributylstannylpyridine (266 mg, 0.72 mmol), $Pd(PPh_3)_2Cl_2$ (6 mg, 0.014 mmol), and LiCl (64 mg, 1.5 mmol) were combined in toluene (5 mL) and degassed by freeze−pump−thaw (5 cycles). The mixture was heated at reflux with stirring for 24 h. After cooling to room temperature, a saturated aqueous solution of KF (10 mL) was added and stirring continued for 1 h. The insoluble residue formed was removed by filtration and washed with toluene. The combined organic solution was evaporated to dryness under reduced pressure, giving a brown residue, which was taken up into dichloromethane (75 mL) and washed with $NaHCO_{3(aq)}$ (1 M, 3 × 50 mL). The organic layer was separated, dried over anhydrous potassium carbonate, and the solvent removed under reduced pressure. The brown residue was purified by chromatography on silica gel, gradient elution from hexane to 70% hexane/30% diethyl ether, giving HL[6] as a colorless oil (48 mg, 45%).

^{1}H NMR ($CDCl_3$, 500 MHz): δ 8.70 (1H, d, ^3J = 5.0, H^6py), 8.37 (1H, t, ^4J = 2.0, H^2), 8.05 (1H, d, ^3J = 2.0, H^5pz), 7.90 (1H, d, ^3J = 7.5, H^4 or H^6), 7.77 (4H, overlapping m, H^3pz, H^3py, H^4py, and H^6 or H^4), 7.55 (1H, t, ^3J = 7.5, H^5), 7.26 (1H, dd, ^3J = 7.0, ^3J = 5.0, H^5py), 6.49 (dd, ^3J = 2.5,^3J = 1.5, H^4pz).

^{13}C{^{1}H} NMR ($CDCl_3$,): δ 156.6 (C^2py), 150.0 (C^6py), 141.4 (C^5pz), 141.0, 140.9, 137.1 (C^4py), 130.1 (C^5py), 127.2 (C^3pz), 125.0 ($C^{2'}$), 122.9, 120.9 (C^3py), 119.9, 117.8, 107.9 (C^4pz). MS (ES^+): *m/z* 222 [M + H^+], 244 [M + Na^+]. HRMS (ES^+): *m/z* 222.0998 [M + H^+]; calcd for $C_{14}H_{12}N_3$, 222.1001.

HL[7] and **HL[8]**, both colorless oils, were prepared similarly: HL[7] from *pre-7*, eluting at 75% hexane/25% diethyl ether in a yield of 74%; HL[8] from *pre-8*, eluting at 70% hexane/30% diethyl ether, in 35% yield.

Data for HL[7]. ^{1}H NMR ($CDCl_3$, 300 MHz): δ 8.70 (1H, d, ^3J = 5.0, H^6py), 8.10 (1H, s, H^2), 8.04 (1H, d, ^3J = 2.5, H^5pz), 7.77 (4H, m, H^3pz, H^3py, H^4py, and H^6 or H^4), 7.63 (1H, s, H^4 or H^6), 7.27 (1H, m overlapping $CHCl_3$, H^5py), 6.48 (1H, m, H^4pz), 2.50 (3H, s). M + H^+: cal 235.28 mes 236.1. HRMS (ES^+) *m/z*: 236.1190 [M+H^+]; calcd for $C_{15}H_{14}N_3$, 236.1188.

Data for HL[8]. ^{1}H NMR ($CDCl_3$, 500 MHz): δ 8.69 (1H, m, H^6py), 7.84 (1H, s, H^6), 7.80 (1H, s, H^2), 7.74 (2H, m, H^3 and H^4py), 7.32 (1H, s, H^4), 7.26 (1H, m, H^5py), 6.00 (1H, s, H^4pz), 2.48 (3H, s, CH_3^{aryl}), 2.34 (3H, s, $CH_3{}^5$pz), 2.31 (3H, s, $CH_3{}^{3pz}$). ^{13}C{^{1}H} NMR ($CDCl_3$): δ 156.9 (C^2py), 149.9 (C^6py), 149.2 (C^3pz),

140.5 (C^3), 139.7 (C^5pz), 137.0 (C^4py), 126.8 (C^6), 126.2 (C^4), 122.7 (C^5py), 121.0 (C^3py), 120.7 (C^2), 107.1 (C^4pz), 21.7 (aryl-CH_3), 13.8 ($CH_3{}^{3pz}$), 12.7 ($CH_3{}^5$pz). MS (ES$^+$) *m/z*: 264 [M + H$^+$], 527 [2M + H$^+$]. HRMS (ES$^+$) *m/z*: 264.14932 [M + H$^+$]; calcd for $C_{17}H_{18}N_3$, 264.14952; 286.13157 [M + Na$^+$] calcd for $C_{17}H_{17}N_3Na$, 286.13147.

1,3-Bis(3-pyrazolyl)benzene HL[9]. Step 1. 1,3-Diacetylbenzene (0.50 g, 3.1 mmol) and *N,N*-dimethylformamide dimethylacetal (DMF-DMA) (1.75 g, 14.7 mmol) in toluene (2 mL) were refluxed for 20 h, to give a yellow precipitate which was filtered off and washed with ether to give the bis-dimethylamino chalcone, ***pre-9***, as a yellow solid (0.60 g, 71%). ^{1}H NMR ($CDCl_3$, 500 MHz): δ 8.40 (1H, s, H^2), 7.99 (2H, dd, ^3J = 7.5, ^4J = 1.5, H^4), 7.82 (2H, d, ^3J = 12.5, C*H*NMe$_2$), 7.46 (1H, t, ^3J = 8.0, H^5), 5.78 (2H, d, ^3J = 12.5, COCH=), 2.94, 3.15 (12H, 2s, NMe$_2$). ^{13}C{^{1}H} NMR ($CDCl_3$): δ 188.6 (C=O), 154.7 (*C*HNMe$_2$), 140.7 (C^1 and C^3), 130.2 (C^4 and C^6), 128.3 (C^3), 126.7 (C^5), 92.6 (CO*C*H=), 45.3, 37.6 (2*C*H$_3$). MS (ES+) *m/z*: 273.3 ([M + H$^+$], 100), 295.2 ([M + Na$^+$], 87), 544.9 ([2M + H$^+$], 20), 566.9 ([2M + Na$^+$], 53). Mp = 172−176 °C.

Step 2. Compound *pre-9* (0.90 g, 3.3 mmol) and hydrazine monohydrate (1.98 g, 39.6 mmol) were dissolved in ethanol (20 mL) and refluxed for 7 h. The solution was evaporated to yield an orange oil which was redissolved in ethanol and dried over $MgSO_4$. Evaporation yielded a white solid which was recrystallized from EtOAc to give HL[9] as a colorless solid (0.45 g, 65%). ^{1}H NMR (*d*$_6$-*acetone*, 300 MHz): δ 12.30 (2H, br, NH), 8.37 (1H, s, H^2), 7.80 (2H, d, ^3J = 7.8, H^4), 7.74 (2H, d, ^3J = 1.8, H^5pz), 7.45 (1H, t, ^3J = 7.8, H^5), 6.78 (2H, d, ^3J = 1.8, H^4pz). ^{13}C{^{1}H} NMR ($CDCl_3$): δ 129.1 (C^2), 124.6 (C^4 and C^6), 122.5 (C^5), 102.2 (C^4pz). MS (ES+) *m/z*: 211 [M + H$^+$], 421 [2M + H$^+$]. Mp = 120−122 °C.

1,3-Bis(3-pyrazolyl-1-phenyl)benzene HL[10]. Ligand HL[9] (0.25 g, 1.2 mmol), iodobenzene (0.73 g, 3.6 mmol), CuI (6.8 mg, 0.012 mmol), K_2CO_3 (0.67 g, 4.8 mmol) and *trans*-1,2-diaminocyclohexane (41 mg, 0.36 mmol) were taken in dioxane (8 mL). The mixture was degassed three times and refluxed under nitrogen for 24 h. The solution turned from blue/green to green/yellow. The solvent was evaporated and the residue taken into CH_2Cl_2 and washed with water. The organic layer was dried over $MgSO_4$, and evaporated to yield a yellow oil (288 mg). The crude product was purified by silica column chromatography, gradient elution from hexane to 30% diethyl ether/70% hexane, to afford HL[10] as a white solid (80 mg, 19%). ^{1}H NMR ($CDCl_3$, 500 MHz): δ 8.43 (1H, s, H^2), 7.99 (2H, d, ^3J = 2.5, H^5pz), 7.92 (2H, dd, ^3J = 8 ^2J = 2, H^4 and H^6), 7.81 (4H, d, ^3J = 8.5, H^2ph), 7.51 (1H, t, ^3J = 8.0, H^5), 7.49 (4H, t, ^3J = 8.5, H^3ph), 7.30 (2H, t, ^3J = 8.5, H^4ph), 6.88 (2H, d, ^3J = 2.5, H^4pz). ^{13}C {^{1}H} NMR ($CDCl_3$, 126 MHz): δ 153.1 (C^1ph), 140.5 (C^3pz), 133.7 (C^1 and C^3), 129.7 (C^3ph), 129.3 (C^5), 128.3 (C^5pz), 126.6 (C^4ph), 125.8 (C^4 and C^6), 123.5 (C^2), 119.4 (C^4 and C^2ph). MS (ES$^+$): *m/z* 363 [M + H$^+$], 385 [M + Na$^+$]. HRMS (ES$^+$): *m/z* 363.16046 [M + H$^+$], calcd for $C_{24}H_{19}N_4$ 363.16042; 385.14235 [M + Na$^+$], calcd for $C_{24}H_{18}N_4Na$ 385.14237. A comparable quantity of the monophenylated product (82 mg) was also recovered when the polarity was increased to 100% diethyl ether (see Supporting Information for data).

1,3-Bis(3-pyrazolyl-1-(4-iodotetrafluorophenyl))benzene HL[11]. This compound was prepared from HL[9] (0.15 g, 0.71 mmol) by the same procedure as that used for HL[10], using iodopentafluorobenzene (0.629 mg, 2.1 mmol) in place of iodobenzene. The product eluted at 90% hexane/10% diethyl ether, to give a colorless solid (43 mg, 8%). ^{1}H NMR ($CDCl_3$, 500 MHz): δ 8.32 (1H, t, ^4J = 1.5, H^2), 7.89 (2H, dd, ^3J = 7.5, ^4J = 1.5, H^4), 7.76 (2H, m, H^5pz), 7.51 (1H, t, ^3J = 7.5, H^5), 6.93 (2H, d, ^3J = 2.5, H^4pz). ^{13}C{^{1}H} NMR ($CDCl_3$, 126 MHz): δ 154.5 (C^3pz), 133.7 (C^5pz), 132.9 (C^1), 129.5 (C^5), 126.6 (C^4), 124.0 (C^2), 106.0 (C^4pz). ^{19}F NMR ($CDCl_3$, 282 MHz): δ −119.1 (4F, m, F^2), 146.0 (4F, dd, F^3). MS (ES$^+$): *m/z* 507 [M − 2I$^-$ + 3H$^+$], 633 [M − I$^-$ + 2H$^+$], 759 [M + H$^+$], 781 [M + Na$^+$]. HRMS (ES$^+$) *m/z*: 758.87967 [M + H$^+$], calcd for $C_{24}H_9N_4F_8{}^{127}I_2$ 758.87835; 780.86126 [M + Na$^+$], calcd for $C_{24}H_8N_4F_8{}^{127}I_2Na$ 780.86030. A large proportion of the monoarylated product (143 mg) was also recovered on increasing the eluent polarity to 1% methanol/99% CH_2Cl_2 (see Supporting Information for data).

Platinum(II) Complexes. The platinum(II) complexes PtL$^{2-4}$Cl and PtL$^{6-7}$Cl were prepared by reaction of the respective ligand HL^n with K_2PtCl_4 (1.1 equiv) in acetic acid (typically 3 mL per 50 mg of ligand). The mixture was first degassed by freeze−pump−thaw (3 cycles), and then heated at reflux with stirring under nitrogen for 3 d. The resulting precipitates, pale colored for PtL$^{2-4}$Cl, yellow for PtL$^{6-7}$Cl, were separated by centrifugation, and washed successively with water, ethanol, and diethyl ether (3 × 10 mL of each). The resulting residue was then extracted into CH_2Cl_2, traces of insoluble residue removed by filtration, and the solvent evaporated under reduced pressure to give the complexes. In the case of PtL[8]Cl, the complexation was carried out by mixing degassed solutions of HL[8] in MeCN and K_2PtCl_4 (1.2 equiv) in H_2O (3:1 ratio by volume), and heating the solution at reflux under nitrogen for 3 d. Work-up was similar to that for the complexes prepared in acetic acid, although no final extraction was required in this case. Yields were typically in the range 40−60%.

PtL^{2}Cl. ^{1}H NMR ($CDCl_3$, 200 MHz): δ 8.02 (4H, overlapping m with satellites, H^3pz and H^5pz), 6.86 (2H, s with satellites, $^4J(^{115}Pt)$ = 8, H^3), 6.62 (2H, t with satellites, ^3J = 2.5, $^4J(^{115}Pt)$ = 9, H^4pz), 2.39 (3H, s, CH_3). MS (ES$^+$): *m/z* 453.0 [M$^+$]. Anal. Calcd for $C_{13}H_{11}ClN_4Pt$: C, 34.4; H, 2.4; N, 12.4%. Found: C, 33.8; H, 2.7; N, 12.1%. HRMS (EI): *m/z* 452.0290, calcd for $C_{13}H_{11}{}^{35}ClN_4{}^{194}Pt$ 452.0293.

PtL^{3}Cl. ^{1}H NMR ($CDCl_3$, 300 MHz): δ 8.04 (2H, d with satellites, ^3J = 3.0, $^4J(^{115}Pt)$ = 13, H^3pz), 7.97 (2H, dd with satellites, ^3J = 2.5, $^3J(^{115}Pt)$ = 10, H^5pz), 7.48 (2H, d, ^3J = 8.0, H^b), 7.27 (2H, d, ^3J = 8.0, H^a), 7.14 (2H, s with satellites, $^4J(^{115}Pt)$ = 7, H^3), 6.60 (2H, dd, ^3J = 3.0, ^3J = 2.5, H^4pz), 2.40 (s, 3H, CH_3). Anal. Calcd for $C_{19}H_{15}ClN_4Pt$: C, 43.1; H, 2.9; N, 10.6%. Found: C, 43.4; H, 3.0; N, 10.1%. MS (ES$^+$, carrier solvent = CH_3CN): *m/z* 535 [MCl$^-$ + CH_3CN].

PtL^{4}Cl. ^{1}H NMR ($CDCl_3$, 200 MHz): δ 8.02 (2H, d, ^3J = 3.0, $^4J(^{115}Pt)$ = 16, H^3pz), 7.91 (2H, d with satellites, ^3J = 2.5, $^3J(^{115}Pt)$ = 13, H^5pz), 7.51 (2H, d, ^3J = 9.0, H^b), 7.08 (2H, s with satellites, $^4J(^{115}Pt)$ = 8, H^3), 6.98 (2H, d, ^3J = 9.0, H^a), 6.56 (1H, t, ^3J = 3.0, ^4J = 2.5, H^4pz), 3.87 (3H, s, CH_3). Anal. Calcd for $C_{19}H_{15}ClN_4OPt$: C, 41.8; H, 2.8; N, 10.3%. Found: C, 42.2; H, 3.0; N, 10.3%. MS (ES$^+$, carrier solvent = CH_3CN): *m/z* 551 [M − Cl$^-$ + CH_3CN]. HRMS (EI): *m/z* 544.0557, calcd for $C_{19}H_{15}{}^{35}ClN_4O^{194}Pt$, 544.0556.

PtL^{6}Cl. $C_{14}H_{10}ClN_3Pt$ ^{1}H NMR ($CDCl_3$, 300 MHz): δ 9.27 (1H, d with satellites, ^3J = 5.5, $^3J(^{115}Pt)$ = 44, H^6py), 8.02 (1H, d with satellites, ^3J = 2.5, $^4J(^{115}Pt)$ = 13, H^3pz), 7.99 (1H, d, ^3J = 2.0, H^5pz), 7.94 (1H, td, ^3J = 8.0, ^4J = 1.5), 7.67 (1H, d with satellites, ^3J = 7.5, $^4J(^{115}Pt)$ = 13, H^3py), 7.30 (2H, overlapping m, H^5py and H^5), 7.19 (1H, t, ^3J = 8.0, H^4), 7.09 (1H, d, ^3J = 8.0, $^4J(^{115}Pt)$ = 11, H^3), 6.62 (1H, t, ^3J = 2.5, H^4pz). Anal. Calcd for $C_{14}H_{10}ClN_3Pt$: C, 37.3; H, 2.2; N, 9.3%. Found: C, 37.5; H, 2.3; N, 9.0%. MS (ES$^+$, carrier solvent = MeOH): *m/z* 447 [M − Cl$^-$ + CH_3OH]$^+$.

PtL^{7}Cl. ^{1}H NMR ($CDCl_3$, 300 MHz): δ 9.31 (1H, d with satellites, ^3J = 5.0, $^3J(^{115}Pt)$ = 44, H^6py), 8.03 and 8.00 (each 1H,

d, ^3J = 2.5, H^{3}pz and H^{5}pz), 7.94 (1H, td, ^3J = 8.0, ^4J = 1.5, H^{4}py), 7.67 (1H, d with satellites, ^3J = 7.5, $^4J(^{115}Pt)$ = 13, H^{3}py), 7.30 (1H, m overlapping with $CHCl_3$, H^{5}py), 7.18 (1H, s, H^5), 6.97 (1H, s with satellites, $^4J(^{115}Pt)$ = 11, H^3), 6.63 (1H, t, ^4J = 2.5, H^{4}pz), 2.38 (3H, s, CH_3). Anal. Calcd for $C_{19}H_{15}ClN_4OPt$: C, 38.8; H, 2.6; N, 9.0%. Found: C, 38.5; H, 3.0; N, 8.5%. MS (ES$^+$, carrier solvent = MeOH): *m*/*z* 461 [M − Cl$^-$ + CH_3OH]$^+$.

PtL^{8}Cl. ^{1}H NMR ($CDCl_3$, 500 MHz): δ 9.51 (1H, d, ^3J = 6.0, $^3J(^{195}Pt)$ = 40, H^{6}py), 7.89 (1H, td, ^3J = 7.0, ^4J = 1.5, H^{4}py), 7.61 (1H, d, ^3J = 8.0, H^{3}py), 7.28 (1H, td, ^3J = 6.5, ^4J = 1.0, H^{5}py), 7.08 (1H, s, H^4), 6.99 (1H, s, H^6), 6.07 (1H, s, H^{4}pz), 2.73, 2.71 (each 3H, s, CH_3^{pz}), 2.34 (3H, s, CH_3^{aryl}). $^{13}C\{^1H\}$ NMR ($CDCl_3$): δ 167.3 (C^{5}py), 155.1 (C^{5}pz), 151.1 (C^{6}py), 142.0 (C^2), 141.6 (C^{3}pz), 138.9 (C^{4}py), 133.4 (C^5), 123.0 (C^{2}py), 120.4 (C^4), 119.3 (C^{3}py), 113.7 (C^6), 108.8 (C^{4}pz), 22.6 (CH_3^{aryl}), 14.7 (CH_3^{pz}), 13.8 (CH_3^{pz}). MS (EI) *m*/*z*: 456 [M − Cl]$^+$, 491 [M$^+$]. HRMS (EI) *m*/*z*: 491.0652 [M$^+$], calcd for $C_{17}H_{16}{}^{35}ClN_3{}^{194}Pt$, 491.0661.

Crystallography. A yellow single crystal of PtL^{6}Cl (0.10 × 0.06 × 0.06 mm) was analyzed at 120(2) K on a Bruker 1000 CCD diffractometer using graphite monochromated Mo Kα radiation (λ = 0.71073 Å). Structure solution was carried out using SHELXS-97[40] and refined by full matrix least-squares in SHELXL-97.[41] All non-hydrogen atoms were refined with anisotropic displacement parameters. Hydrogen atoms were positioned geometrically with isotropic displacement parameters fixed to ride on the parent atom (aromatic C−H 0.94 Å, U_{iso} = 1.2 × U_{eq}(C); methyl C−H 0.98 Å, U_{iso} = 1.5 × U_{eq}(C)). The asymmetric unit consisted of two molecules. The L^6 ligand in the second molecule was disordered over two orientations, depending which side the pyrazole ring is on; the orientations were modeled at occupancies of 60:40 and the geometry was constrained to be the same as that of the ordered ligand in the asymmetric unit. Crystal data: M = 464.82, monoclinic space group $P2_1/n$, a = 16.8287(13), b = 8.8822(7), c = 18.3338(14) Å, β = 92.968(1), V = 2736.8(4) Å^3, Z = 8, D_c = 2.256 Mg/m^3, μ = 10.441 mm^{-1}, $F(000)$ = 1744, 25639 reflections collected ($1.60 \le \theta \le 26.37°$), 5586 independent reflections (R_{int} = 0.0618) were used for structure refinement, final R_1 = 0.0405 [$F^2 > 2\sigma(F)$], wR_2 = 0.0624 [$F^2 > 2\sigma(F)$], R_1 = 0.0619 (all data), wR_2 = 0.0666 (all data), GOF (F^2) = 1.148, largest peak, hole = 1.072, −0.932 e Å^{-3}. Crystallographic data in CIF format is provided as Supporting Information.

Photophysical Measurements. Absorption spectra were measured on a Biotek Instruments XS spectrometer, using quartz cuvettes of 1 cm path length. Steady-state luminescence spectra were measured using a Jobin Yvon FluoroMax-2 spectrofluorimeter, fitted with a red-sensitive Hamamatsu R928 photomultiplier tube; the spectra shown are corrected for the wavelength dependence of the detector, and the quoted emission maxima refer to the values after correction. Samples for emission measurements were contained within quartz cuvettes of 1 cm path length modified with appropriate glassware to allow connection to a high-vacuum line. Degassing was achieved via a minimum of three freeze−pump−thaw cycles while connected to the vacuum manifold; final vapor pressure at 77 K was $<5 \times 10^{-2}$ mbar, as monitored using a Pirani gauge. Luminescence quantum yields were determined by the method of continuous dilution, using quinine sulfate in 1 M H_2SO_4 as the standard (ϕ = 0.546 [42]); estimated uncertainty in ϕ is ± 20% or better.

The luminescence lifetimes of the complexes were measured by time-correlated single-photon counting, following excitation at 374.0 nm with an EPL-375 pulsed-diode laser. The emitted light was detected at 90° using a Peltier-cooled R928 PMT after passage through a monochromator. The estimated uncertainty in the quoted lifetimes is ± 10% or better. Lifetimes at 77 K in excess of 10 μs were measured by multichannel scaling following excitation with a μs-pulsed xenon lamp; an excitation wavelength of 374 nm (band-pass 5 nm) was selected with a monochromator. Bimolecular rate constants for quenching by molecular oxygen, k_Q, were determined from the lifetimes in degassed and air-equilibrated solution, taking the concentration of oxygen in CH_2Cl_2 at 0.21 atm O_2 to be 2.2 mmol dm^{-3}.[43]

Acknowledgment. We thank EPSRC (EP/D500265/1) and the University of Durham for financial support, Professor J.A.K. Howard for access to crystallography facilities, Dr. H. Sparkes for assistance, and the EPSRC National Mass Spectrometry Service Centre for providing EI and CI spectra of platinum(II) complexes.

Supporting Information Available: Further details of synthesis and characterization of ligands and intermediates; frontier orbital plots of the complexes, obtained by DFT calculations; absorption and emission spectra of the complexes in different solvents overlaid; crystallographic data for PtL^{7}Cl in CIF format. This material is available free of charge via the Internet at http://pubs.acs.org.

IC8014157

(40) Sheldrick, G. M. *Acta Crystallogr.* **1990**, *A46*, 467.
(41) Sheldrick, G. M. *Computer Program for Crystal Structure Refinement*; University of Göttingen: Göttingen, Germany.
(42) Meech, S.; Phillips, D. *J. Photochem.* **1983**, *23*, 193.
(43) Murov, S. L.; Carmichael, I.; Hug, G. L. *Handbook of Photochemistry*, 2nd ed.; Marcel Dekker: New York, 1993.